
BAYESIAN MODAL REGRESSION BASED ON MIXTURE DISTRIBUTIONS

A PREPRINT

• **Qingyang Liu**
 Department of Statistics
 University of South Carolina
 Columbia, SC 29201
 qingyang@email.sc.edu

• **Xianzheng Huang**
 Department of Statistics
 University of South Carolina
 Columbia, SC 29201
 huang@stat.sc.edu

• **Ray Bai**
 Department of Statistics
 University of South Carolina
 Columbia, SC 29201
 rbai@mailbox.sc.edu

November 19, 2022

ABSTRACT

Compared to mean regression and quantile regression, the literature on modal regression is very sparse. We propose a unified framework for Bayesian modal regression based on a family of unimodal distributions indexed by the mode along with other parameters that allow for flexible shapes and tail behaviors. Following prior elicitation, we carry out regression analysis of simulated data and datasets from several real-life applications. Besides drawing inference for covariate effects that are easy to interpret, we consider prediction and model selection under the proposed Bayesian modal regression framework. Evidence from these analyses suggest that the proposed inference procedures are very robust to outliers, enabling one to discover interesting covariate effects missed by mean or median regression, and to construct much tighter prediction intervals than those from mean or median regression. Computer programs for implementing the proposed Bayesian modal regression are available at https://github.com/rh8liuqy/Bayesian_modal_regression.

Keywords Mode · Heavy-tailed distribution · Outlier · Unimodal distribution

1 Introduction

There is an abundance of literature on mean regression models which model the conditional mean of a response variable Y given a set of covariates \mathbf{X} . However, it is no secret that the mean is sensitive to outliers. Median regression – or more generally, quantile regression – is robust to outliers and is thus an appealing alternative to mean regression [Koenker et al., 2017]. Besides the mean and median, the mode is yet another commonly used measure of central tendency. Compared with mean or median regression, modal regression concerns the conditional *mode* of Y given \mathbf{X} and is much less explored [Sager and Thisted, 1982, Lee, 1989, 1993], especially in the parametric framework.

But why are modal regression models useful additions to the well-established mean and median regression models? For unimodal and asymmetric distributions, intervals around the conditional mode typically have higher coverage probability than intervals of the same length around the conditional mean or median [Yao and Li, 2014]. Consequently, prediction intervals from modal regression tend to be narrower than those for mean or median regression when data arise from a unimodal and skewed distribution. By construction, modal regression explores the relationship between the “most probable” value of Y given \mathbf{X} , and thus offers a highly interpretable representative value of the response. Thanks to the nature of the mode, modal regression is extremely robust to outliers that can obscure some inherent covariate effect suggested by the majority of observations, making it a worthy rival of median regression as an alternative to mean regression in regard to feature discovery.

A major challenge in building parametric modal regression models is constructing an appropriate distribution family that subsumes asymmetric, symmetric, light-tailed, and fat-tailed distributions. In this paper, we propose the general unimodal distribution (GUD) family, which is a subfamily of the general two-component mixture distribution family described in Section 3. Members of the GUD family have a location parameter as the mode, in addition to shape and

scale parameters that control the skewness and tail behaviors. Thus, our framework is appropriate for both asymmetric *and* symmetric conditional distributions, as well as both light-tailed *and* heavy-tailed distributions. In the extreme case, our framework can also model data from distributions without any finite moments, which we introduce in Section 3.3. We propose to estimate the conditional mode and the shape/scale parameters using a Bayesian approach. By placing appropriate prior distributions on model parameters, our modal regression models can be implemented straightforwardly using Markov chain Monte Carlo (MCMC) and provide natural uncertainty quantification through the posterior distributions.

1.1 Existing Work on Modal Regression

Frequentist nonparametric modal regression has been the mainstream in the limited existing literature on modal regression (see [Chen \[2018\]](#) for a comprehensive review). The higher statistical efficiency and greater interpretability of covariate effects under a parametric framework motivate some recent development in frequentist parametric modal regression. For example, [Aristodemou \[2014\]](#) and [Bourguignon et al. \[2020\]](#) proposed a parametric modal regression model based on a gamma distribution for a positive response; [Zhou and Huang \[2020\]](#) proposed two parametric modal regression models for a bounded response. [Menezes et al. \[2021\]](#) give a nice review on these and other parametric modal regression models for a bounded response. In contrast to these existing parametric modal regression models for *bounded* data, the modal regression models in the present manuscript are based on a *new* GUD family whose support is the *entire* real line. Furthermore, our work deals with *Bayesian* inference for modal regression.

The literature on Bayesian modal regression is even more sparse. [Yu and Aristodemou \[2012\]](#) proposed a nonparametric Bayesian modal regression model using Dirichlet process mixtures of uniform distributions. [Zhou and Huang \[2022\]](#) proposed a parametric Bayesian modal regression model based on a four-parameter beta distribution whose support is bounded yet unknown. [Damien et al. \[2017\]](#) introduced a more flexible parametric form of Bayesian modal regression using mixtures of triangular densities for a response with an unknown bounded support. Remaining in the parametric framework, a major strength of our proposed GUD family is that it naturally facilitates data-driven learning of the skewness and tails of the underlying distribution supported on the entire real line, while signifying the mode as the central tendency measure of the response.

1.2 Our Contributions

This paper aims to widen the scope of Bayesian modal regression models and highlight the advantages of these models through analyses of datasets from real-life applications in several disciplines. We provide a unified framework of Bayesian modal regression models based on the GUD family that contains a large variety of unimodal distributions. We adopt the fully Bayesian approach via MCMC, so that inference of the conditional mode does not rely on asymptotic approximations. Our method is shown to provide reliable inference in small sample sizes. The fully Bayesian approach also comes with a convenient way of constructing prediction intervals from the posterior predictive distribution that is approximated using a simple random number generation algorithm for the GUD family. Indeed, the convenience in data generation via a data augmentation trick (to be discussed on Section 3) is yet another advantage of the GUD family. Finally, we exploit the model criterion known as the Bayesian leave-one-out expected log predictive density for model selection to help practitioners choose an appropriate distribution for their final analysis.

The main contributions of this paper can be summarized as follows:

1. We propose the GUD family that is suitable for Bayesian modal regression. The GUD family contains distributions that are symmetric or asymmetric, (non)normal, and/or fat-tailed.
2. We formulate rules of prior elicitation for the GUD family. In particular, we place a flat prior on regression coefficients, weakly informative priors on all other model parameters, and establish posterior propriety under mild conditions.
3. We provide strategies for constructing prediction intervals and for selecting an appropriate likelihood for Bayesian modal regression analysis.
4. We illustrate the following benefits of our proposed Bayesian modal regression framework through simulation studies and data applications in economics, criminology, environmental science, and molecular biology: a) robustness to outliers, b) more precise prediction, and c) high interpretability of covariate effects.

The structure of this paper is as follows. In Section 2, we motivate our proposed Bayesian modal regression framework with two data applications. In Section 3, we formally define the GUD family and zoom in on several important members in the family. Section 4 introduces Bayesian inference for these modal regression models, including prior elicitation, uncertainty quantification, and model selection. Section 5 provides simulation studies that illustrate the strengths of our

methodology. In Section 6, we provide two additional data applications from environmental science and molecular biology. Section 7 concludes the paper with some remarks about our Bayesian modal regression framework and some directions for future research.

2 Motivating applications

As a prelude to introducing our Bayesian modal regression framework, we first present results from applying the proposed methodology (to be elaborated in Sections 3 and 4) to datasets from the economics and the criminology literature.

2.1 Modeling highly right-skewed bank deposits

It is common knowledge to economists that wealth distributions are highly skewed to the right [Benhabib and Bisin, 2018]. The cumulative nature of wealth not only has impact on individuals' net worth, but also has an influence on assets of large companies, including bank holding companies. In this example, we analyzed the deposits data of 50 banks and savings institutions in the United States on July 2, 2010 (Table 3.4.1 in Siegel [2016]).

Figure 1 presents the estimated density plot that results from fitting an intercept-only regression model based on the Double Two-Piece-Student- t , or DTP-Student- t , distribution (to be introduced in Section 3) to the dataset, along with the histogram of the underlying data. From this figure, we can see that the estimated mode using the DTP-Student- t distribution is close to the nonparametric mode estimate based on the histogram. This similarity and the close resemblance of the fitted density to the shape of the histogram indicate that the DTP-Student- t distribution is an adequate choice for the bank deposits data.

The other two measures of central tendency, i.e. the sample mean and median, are both shown to be larger than the estimated parametric mode in Figure 1. The sample mean, which equals 92.6 billion dollars, is obviously not a good measure of central tendency for most large banks and savings institutions in the United States. In particular, 40 of the 50 banks and savings institutions in our dataset had deposits *less* than 92.6 billion dollars on July 2, 2010. The sample median for this data is 40.5 billion dollars, indicating that 50% of banks in the dataset had deposits larger than 40.5 billion dollars while the other half had deposits smaller than 40.5 billion dollars. Despite of its high interpretability, the (sample) median is usually difficult to visualize either from a density plot or a histogram. In contrast, it is much easier for data analysts to locate and interpret the mode than the mean or median in Figure 1. The estimated mode using the DTP-Student- t distribution is where the density plot reaches its peak, and is close to where the histogram reaches to its peak. More specifically, the posterior mean of the mode is 20 billion dollars, suggesting that banks in the United States are *most likely* to have deposits of around 20 billion dollars during that time.

2.2 Modal versus mean and median regression for analyzing murder rates

As a second motivating example, we analyze a dataset from Agresti et al. [2021] containing the murder rate, percentage of college education, poverty percentage and metropolitan rate for the 50 states in the United States and the District of Columbia (D.C.) from 2003. The murder rate is defined as the annual number of murders per 100,000 people in the population. The poverty percentage is the percentage of the residents with income below the poverty level, and the metropolitan rate is defined as the percentage of population living in the metropolitan area.

At the stage of exploratory data analysis, we plotted the conditional scatter plot matrices of the U.S. crime data in Figure 2. From the first row of the conditional scatter plot matrices, a positive association between the poverty percentage and murder rate, and also a positive association between the metropolitan rate and murder rate are relatively evident; but an association between the college percentage and murder rate is harder to perceive in the figure. Figure 2 also brings up a clear outlier, which is D.C. *Without* this outlier, there appears to exist a negative association between the college percentage and murder rate.

To formally investigate the association between the murder rate (Y) and the aforementioned variables, we fit the following models to the U.S. crime dataset:

$$\mathbb{M}(Y \mid \beta) = \beta_0 + \beta_1 \times \text{college} + \beta_2 \times \text{poverty} + \beta_3 \times \text{metropolitan},$$

where $\mathbb{M}(\cdot)$ generically refers to the conditional mean, median, or mode. Table 1 presents the inference results from mean/median/modal regression models. All three models share some conclusions in common. Namely, all models determined that there were positive associations between the poverty percentage and murder rate and between the metropolitan rate and murder rate. However, with a posterior credible interval (CI) of (0.20, 0.74), the mean regression model (specified by (14)) implies that there exists a *positive* association between the college percentage and crime

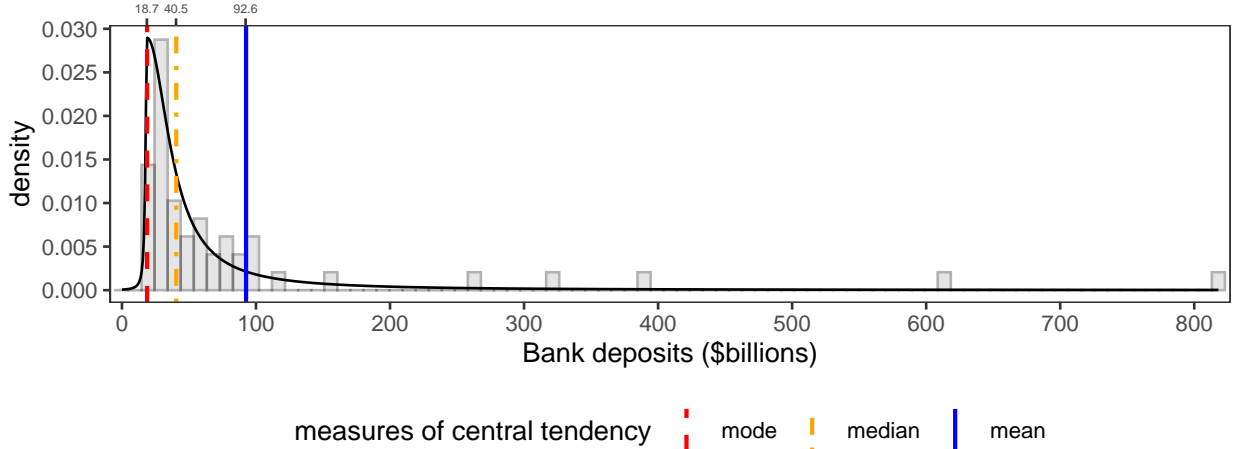


Figure 1: Deposits (in billions of dollars) of 50 banks and savings institutions in the United States on July 2, 2010. The solid black curve is the estimated density of the DTP-Student- t distribution. The three vertical lines mark locations of the sample mean (blue solid line), the sample median (orange dot-dashed line), and the estimated mode (red dashed line), respectively.

rate, conditionally on the other covariates in the model. We believe that this inference result is difficult to justify, in light of existing results from the criminology literature that conclude a negative association between higher education attainment and crime [Lochner, 2020, Hjalmarsson and Lochner, 2012]. On the other hand, with a CI of $(-0.27, 0.05)$, the Bayesian median regression model (formulated in (15)) concludes that the college percentage is *not* significantly associated with the murder rate, conditionally on the other covariates. Our Bayesian modal regression model with the Two-Piece scale-Student- t , or TPSC-Student- t , distribution (to be introduced in Section 3) draws a different conclusion. With a CI of $(-0.33, -0.06)$, our Bayesian modal regression model concludes that there is a *negative* association between the college percentage and the murder rate, which is more consistent with findings from the criminology literature. Lastly, according to the model criterion referred to as the expected log predictive density (ELPD, introduced in Section 4.2) in Table 1, the modal regression model based on the TPSC-Student- t likelihood yields the highest value of ELPD, indicating a better fit for the data than the mean and median regression models.

We repeated the above analyses after removing the D.C. outlier from the data. Now the median and modal regression models do in fact suggest a negative association between the college percentage and murder rate, whereas the mean regression model insists on lack of significant association between them. This exercise demonstrates that modal regression based on the proposed GUD family can be even more robust to outliers than median regression, and has a stronger potential in drawing reliable inferences and unveiling important features of data even in the presence of extreme outliers.

3 Family of general unimodal distributions

Having motivated our Bayesian modal regression framework and demonstrated its benefits on two real-life applications in Section 2, we now formally introduce the GUD family for Bayesian modal regression.

The probability density function (pdf) of a member of the GUD family is in the form a mixture of two pdfs, f_1 and f_2 , given by

$$f(y | w, \theta, \sigma_1, \sigma_2) = w f_1(y | \theta, \sigma_1) + (1 - w) f_2(y | \theta, \sigma_2). \quad (1)$$

In the mixture pdf (1), $w \in [0, 1]$ is the weight parameter, $\theta \in (-\infty, +\infty)$ is the mode as the only location parameter in (1), σ_1 consists of parameters other than the location parameter in the pdf $f_1(\cdot | \theta, \sigma_1)$, and σ_2 is defined similarly for $f_2(\cdot | \theta, \sigma_2)$. Clearly, the GUD family belongs to the more general two-component mixture distribution family. One feature of GUD that makes it stand out from the bigger family of two-component mixture distributions is that the two component distributions of GUD share the same location parameter θ as the mode, a feature that makes GUD especially suitable for modal regression. In contrast, a two-component normal mixture for instance, as a widely referenced member in the bigger family, can be multimodal, and it is non-trivial to impose constraints on two normal components

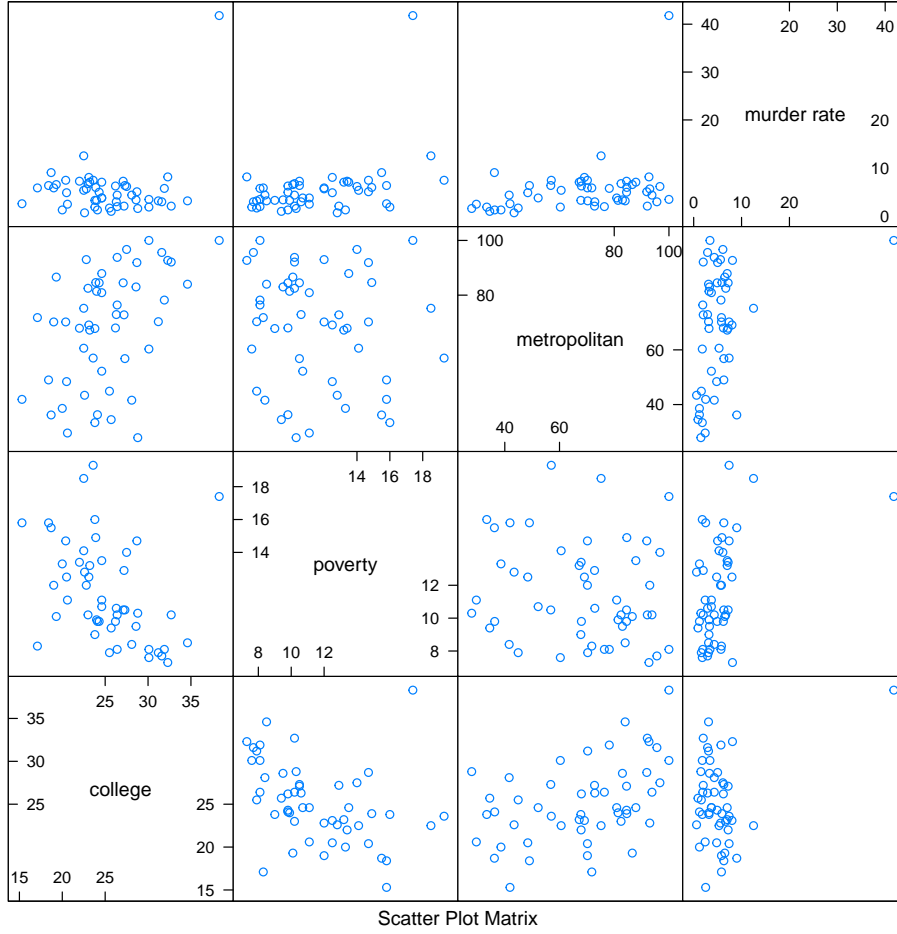


Figure 2: The conditional scatter plot matrices of the U.S. crime data

to guarantee unimodality [Sitek, 2016]. Even after formulating a unimodal normal mixture, its mode may not have an analytical form [Behboodian, 1970]. Many other members in the more general two-component mixture distribution family have the same pitfalls.

Besides unimodality, we reiterate and complement the following three restrictions on (1) to make the GUD family suitable and convenient for modal regression:

- (R1) The pdfs $f_1(\cdot \mid \theta, \sigma_1)$ and $f_2(\cdot \mid \theta, \sigma_2)$ are unimodal at θ .
- (R2) The pdfs $f_1(\cdot \mid \theta, \sigma_1)$ and $f_2(\cdot \mid \theta, \sigma_2)$ are left-skewed and right-skewed respectively.
- (R3) The mixture pdf $f(\cdot \mid w, \theta, \sigma_1, \sigma_2)$ in (1) is continuous in its domain.

Restriction (R1) is already implied earlier when we stress that the two components in (1) share the same location parameter θ as the finite mode. In the context of modal regression, (R1) ensures that one can easily link a linear predictor $X^\top \beta$ with the conditional mode of Y . Because modal regression adds more value to mean/median regression when data are skewed and contain outliers, we impose (R2) to make members in GUD exhibit a wide range of skewness and tail behaviors. This second restriction also solves the notorious label switching problem that many other two-component mixture distributions suffer from, because $f_1(\cdot \mid \theta, \sigma_1)$ and $f_2(\cdot \mid \theta, \sigma_2)$ satisfying (R2) must come from different distribution families in some strict sense, as opposed to, say, both coming from the normal family. According to Theorem 1 of Teicher [1963], this guarantees identifiability of all parameters associated with GUD. Lastly, (R3) eliminates ill-constructed pdfs whose mode may occur at a jump discontinuity.

Table 1: The estimates of the covariate effects for the mean/median/modal regression models fit to the U.S. crime data set. The mean, 5% quantile, and 95% quantile of the posterior distribution of each covariate effect are listed under Mean, q5, and q95, respectively. ELPD stands for expected log predictive density.

Regression model	ELPD	Parameter (covariate)	Mean	q5	q95
Mean regression	-162.59	β_1 (college)	0.47	0.20	0.74
		β_2 (poverty)	1.14	0.76	1.51
		β_3 (metropolitan)	0.07	0.01	0.12
Median regression	-133.12	β_1 (college)	-0.12	-0.27	0.05
		β_2 (poverty)	0.44	0.22	0.67
		β_3 (metropolitan)	0.06	0.03	0.08
Modal regression	-123.27	β_1 (college)	-0.20	-0.33	-0.06
		β_2 (poverty)	0.24	0.01	0.46
		β_3 (metropolitan)	0.06	0.04	0.09

Henceforth, when a random variable Y follows a distribution in the GUD family, we state that $Y \mid w, \theta, \sigma_1, \sigma_2 \sim \text{GUD}(w, \theta, \sigma_1, \sigma_2)$. Like for other two-component mixture distributions, one may view $Y = ZX_1 + (1 - Z)X_2$, where $X_1 \mid \theta, \sigma_1 \sim f_1(\cdot \mid \theta, \sigma_1)$, $X_2 \mid \theta, \sigma_2 \sim f_2(\cdot \mid \theta, \sigma_2)$, and $Z \mid w \sim \text{Bernoulli}(w)$, with Z , X_1 , and X_2 independent. This viewpoint gives rise to a data augmentation method outlined below for generating data from a GUD effortlessly:

- (i) Sample $X_1 \mid \theta, \sigma_1 \sim f_1(\cdot \mid \theta, \sigma_1)$.
- (ii) Sample $X_2 \mid \theta, \sigma_2 \sim f_2(\cdot \mid \theta, \sigma_2)$.
- (iii) Sample $Z \mid w \sim \text{Bernoulli}(w)$.
- (iv) $Y \leftarrow ZX_1 + (1 - Z)X_2$.

Having an efficient random number generation method is especially beneficial in constructing Bayesian prediction intervals, since the most common way to approximate the posterior predictive density is by drawing samples from the posterior predictive distribution during the MCMC iterations. We will continue our discussion about the Bayesian prediction intervals in Section 4.2.

Relating to existing literature, the GUD family *subsumes* several previously proposed distributions, such as those introduced in Fernández and Steel [1998] and Rubio and Steel [2015], as special cases. In what follows, we detail several examples of distributions from the GUD family.

3.1 The flexible Gumbel distribution

For predicting extreme events, the Gumbel distribution is a popular choice in many fields such as hydrology, earthquake forecasting, and insurance [Smith, 2003, Vidal, 2014, Shin et al., 2015]. The pdf of the Gumbel distribution for the maximum is

$$f_{\text{Gumbel}}(y \mid \theta, \sigma) = \frac{1}{\sigma} \exp \left\{ -\frac{y - \theta}{\sigma} - \exp \left(-\frac{y - \theta}{\sigma} \right) \right\} \mathbb{I}(-\infty < y < \infty),$$

where $\theta \in \mathbb{R}$ is the mode as the location parameter, $\sigma > 0$ is the scale parameter, and $\mathbb{I}(\cdot)$ is the indicator function. To describe data that contains a mix of extremely large and extremely small events, Liu et al. [2022] proposed the flexible Gumbel (FG) distribution specified by the pdf

$$f_{\text{FG}}(y \mid w, \theta, \sigma_1, \sigma_2) = w f_{\text{Gumbel}}(-y \mid -\theta, \sigma_1) + (1 - w) f_{\text{Gumbel}}(y \mid \theta, \sigma_2). \quad (2)$$

Mapping to (1), we have $f_1(y \mid \theta, \sigma_1) = f_{\text{Gumbel}}(-y \mid -\theta, \sigma_1)$ as the pdf of the left-skewed Gumbel distribution for the minimum, and $f_2(y \mid \theta, \sigma_2) = f_{\text{Gumbel}}(y \mid \theta, \sigma_2)$ as the pdf of the right-skewed Gumbel distribution for the maximum. We illustrate Bayesian modal regression based on the FG likelihood in Section 6.2. The FG distribution serves as a good choice of likelihood if the data is a mixture of extreme events, such as monthly maximum/minimum water elevation changes, and weekly heaviest/lightest traffic on a highway.

3.2 The Double Two-Piece distribution

Rubio and Steel [2015] defined the Double Two-Piece (DTP) distribution by mixing two truncated distributions. For a pdf belonging to some location-scale family of the form $(1/\sigma)f((y - \theta)/\sigma \mid \delta)$ that is unimodal at θ , with a scale parameter $\sigma > 0$ and a shape parameter δ , the pdf of the corresponding left θ -truncated distribution is

$$f_{LT}(y \mid \theta, \sigma, \delta) = \frac{2}{\sigma} f\left(\frac{y - \theta}{\sigma} \mid \delta\right) \mathbb{I}(y < \theta), \quad (3)$$

and the corresponding right θ -truncated distribution is specified by the following pdf,

$$f_{RT}(y \mid \theta, \sigma, \delta) = \frac{2}{\sigma} f\left(\frac{y - \theta}{\sigma} \mid \delta\right) \mathbb{I}(y \geq \theta). \quad (4)$$

By mixing the pdfs in (3)-(4), we obtain the DTP pdf as

$$f_{DTP}(y \mid \theta, \sigma_1, \sigma_2, \delta_1, \delta_2) = w f_{LT}(y \mid \theta, \sigma_1, \delta_1) + (1 - w) f_{RT}(y \mid \theta, \sigma_2, \delta_2), \quad (5)$$

where

$$w = \frac{\sigma_1 f(0; \delta_2)}{\sigma_1 f(0; \delta_2) + \sigma_2 f(0; \delta_1)} \quad (6)$$

as the weight chosen to produce a mixture distribution that satisfies (R3). Restrictions (R1) and (R2) are trivially satisfied by the construction of the left/right θ -truncated pdfs in (3)-(4). Thus, DTP distributions belong to the GUD family. Note, however, that our general GUD family (1) does not *require* the two component densities to be truncated, as we demonstrated earlier with the FG distribution (2).

As a concrete example, consider the location-scale family as the three-parameter Student's t distributions, i.e., the non-standardized Student's t distributions, with location parameter θ , scale parameter $\sigma > 0$, and continuous degree of freedom $\delta > 0$ [Geweke, 1993]. Following (3) and (4), one has the corresponding left-skewed truncated three-parameter Student's t distribution and the right-skewed truncated three-parameter Student's t distribution, respectively. This leads to the distribution defined according to (5) and (6) that we call the DTP-Student- t distribution. The DTP distribution family contains numerous distributions, all of which are suitable for modal regression (see Rubio and Steel [2015] for more). In the sequel, we concentrate on the DTP-Student- t distribution as a special member of the DTP distribution.

3.3 The Two-Piece scale distribution

By setting $\delta_1 = \delta_2 = \delta$ in (5), one obtains the pdf of a subfamily of the DTP family proposed in Fernández and Steel [1998], referred to as the two-piece scale (TPSC) distribution family,

$$f_{TPSC}(y \mid w, \theta, \sigma, \delta) = w f_{LT}\left(y \mid \theta, \sigma \sqrt{\frac{w}{1-w}}, \delta\right) + (1 - w) f_{RT}\left(y \mid \theta, \sigma \sqrt{\frac{1-w}{w}}, \delta\right). \quad (7)$$

We shall point out that, in Fernández and Steel [1998], a shape parameter $\gamma = w^{0.5}(1-w)^{-0.5}$ is used instead of the weight parameter w when formulating the mixture pdf. We adopt the parameterization in (7) because we find it more straightforward to elicit a noninformative prior for w than placing a noninformative prior on γ .

Similar to the construction of the DTP-Student- t distribution, we can construct the TPSC-Student- t distribution by choosing the two component distributions to be the left and right θ -truncated three-parameter Student's t distributions. When $w = 0.5$, the TPSC-Student- t distribution converges to a normal distribution with mean θ and standard deviation σ as $\delta \rightarrow \infty$; and it reduces to a Cauchy distribution with mode θ and scale parameter σ when $\delta = 1$. Hence, even as a special case of the DTP-Student- t distribution, the TPSC-Student- t distribution is flexible enough to describe normally distributed data and non-normal data with extreme outlier(s) from distributions that do not have any finite moments. Since the TPSC-Student- t has fewer parameters than the DTP-Student- t distribution, it is an adequate choice for small datasets. On the other hand, the DTP-Student- t distribution may be preferred when there is moderate sample size. Certainly, one can conduct several rounds of modal regression analysis assuming different unimodal distributions for the response, such as the FG, DTP-Student- t , and TPSC-Student- t distributions, and then select the most appropriate model using the model selection criteria that we introduce in Section 4.2. All of these models can be easily implemented using the code developed for this work.

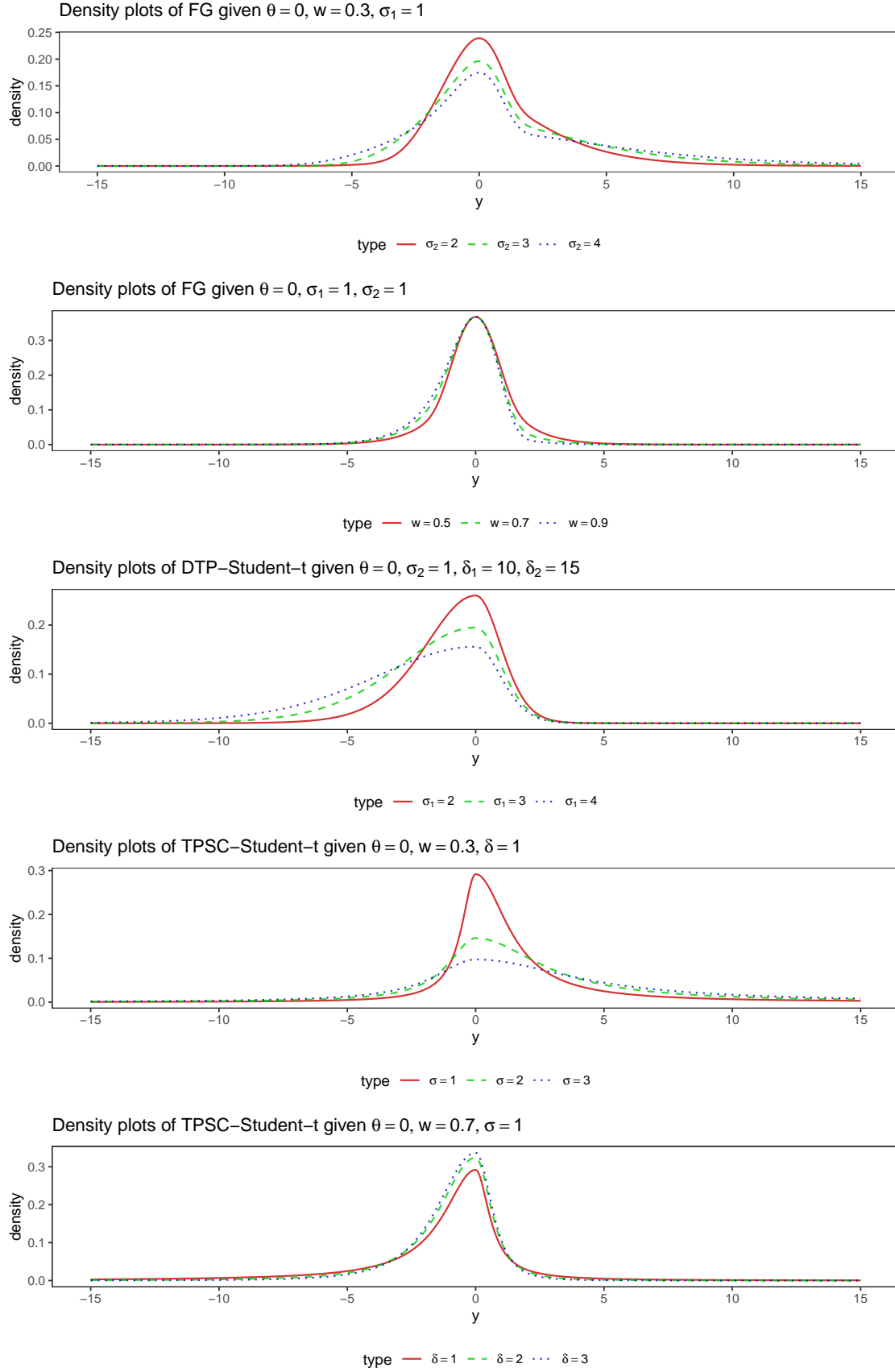


Figure 3: Density plots of different distributions in the GUD family with different parameter specifications.

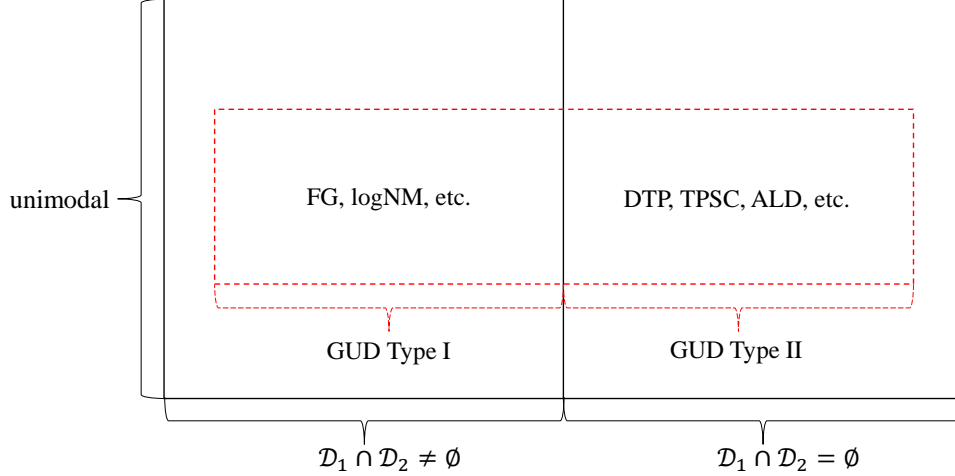


Figure 4: Venn diagram of the unimodal two-components mixture distributions.

3.4 Type I GUD and type II GUD subfamilies

As illustrated in the preceding three subsections, the GUD family is a *generalization* of several previously proposed unimodal two-component mixture distributions. Figure 3 presents pdfs of FG, DTP-Student- t , and TPSC-Student- t distributions with different parameter specifications, which encompass asymmetric, symmetric, fat-tailed, and thin-tailed densities. In particular, the first panel in Figure 3 presents the density plot of FG distribution with varying scale parameters of the right-skewed component. As σ_2 becomes larger, the tails of FG distribution (especially the right tail) become fatter. In the second panel, we show that the FG distribution is symmetric if $w = 0.5$ and $\sigma_1 = \sigma_2$. With the increase of weight parameter $w > 0.5$, the pdf of FG distribution puts more weight on the left-skewed part, therefore, becomes more left-skewed. In the third panel, with the increase of σ_1 , the scale parameter of left-skewed component, the pdf of DTP-Student- t distribution has a fatter left tail, has the almost same right tail, and becomes more left-skewed. The fourth panel shows the drastic change in shape of the pdf for the TPSC-Student- t distribution given different choices of scale parameter σ , which is shared by both mixture components. The last panel presents the subtle changes of the tail behaviors of the TPSC-Student- t distribution given different choices of degree of freedom δ , which is shared by both the left-skewed and the right-skewed components.

We now describe how our broadly defined GUD family can be further categorized into two subfamilies. Let \mathcal{D}_1 and \mathcal{D}_2 denote the domains of $f_1(\cdot | \theta, \sigma_1)$ and $f_2(\cdot | \theta, \sigma_2)$ in the GUD pdf (1) respectively. If $\mathcal{D}_1 \cap \mathcal{D}_2 \neq \emptyset$, we call the mixture distribution the *type I GUD*. The FG distribution is an example of type I GUD. In Appendix B, we present the construction of the lognormal mixture distribution (logNM), which is another example of type I GUD. On the other hand, if $\mathcal{D}_1 \cap \mathcal{D}_2 = \emptyset$, then we have the *type II GUD*. The DTP distributions and the asymmetric Laplace distribution [ALD, Koenker and Machado, 1999] belong to this subfamily of type II GUD. Figure 4 presents the partition of the GUD family into type I and type II GUD subfamilies.

4 Bayesian modal regression

Having defined the GUD family in Section 3, we are now in a position to introduce our Bayesian modal regression framework. In the remainder of the manuscript, we assume that we observe n independent pairs of observations $(\mathbf{X}_1, Y_1), (\mathbf{X}_2, Y_2), \dots, (\mathbf{X}_n, Y_n)$. Here, $\mathbf{X}_i = (X_{i1}, \dots, X_{ip})^\top$ denotes a vector of p covariates for the i th observation. We assume exchangeability in the sense that, given $\mathbf{X} = (\mathbf{X}_1, \dots, \mathbf{X}_n)$ and all parameters, n observations in $\mathbf{Y} = (Y_1, \dots, Y_n)$ are independent. Our goal is to conduct inference about the conditional *mode* of the response variable Y given the covariates \mathbf{X} .

4.1 Prior elicitation

For all modal linear regression models in this paper, we assume that, for $i = 1, \dots, n$,

$$Y_i | \mathbf{X}_i, w, \beta, \sigma_1, \sigma_2 \sim \text{GUD}\left(w, \mathbf{X}_i^\top \beta, \sigma_1, \sigma_2\right), \quad (8)$$

where GUD generically refers to a member of the GUD family. Recall that any member of the GUD family contains the location parameter as its mode, which is $\mathbf{X}_i^\top \beta$ as the conditional mode for Y_i given \mathbf{X}_i in (8).

To conduct inference for our model in (8), we adopt a Bayesian approach where appropriate priors are placed on the model parameters $(w, \beta, \sigma_1, \sigma_2)$. We endow the weight parameter w with a noninformative $\text{Uniform}(0, 1)$ prior, and use weakly informative $\text{InverseGamma}(1, 1)$ or $\text{InverseGamma}(5, 5)$ priors for all positive parameters in σ_1 and σ_2 . As pointed out by Diebolt and Robert [1994], improper priors usually lead to improper posterior distributions for mixture distributions because of identifiability problems. Therefore, if $\sigma_1 \cap \sigma_2 = \emptyset$, then improper priors should *not* be used for σ_1 or σ_2 . In Appendix B, we prove that using an improper prior for any of the parameters in σ_1 or σ_2 can lead to an improper posterior distribution.

On the other hand, a flat prior $p(\beta) \propto 1$ on the regression coefficients β usually leads to a proper posterior distribution because both right and left skewed components share the same location parameter. In Section A of the Appendix, we provide sufficient conditions under which a flat prior can be used for β such that the posterior distribution is proper. These sufficient conditions are very mild and are likely to be satisfied in practice. All models going forward thus use a noninformative flat prior, $p(\beta) \propto 1$, for β .

Revisiting the three members of the GUD family discussed in Section 3, we have the Bayesian modal linear regression model based on the FG likelihood (2) formulated as follows,

$$\begin{aligned} Y_i | \mathbf{X}_i, w, \beta, \sigma_1, \sigma_2 &\sim \text{FG} \left(w, \mathbf{X}_i^\top \beta, \sigma_1, \sigma_2 \right), \\ w &\sim \text{Uniform}(0, 1), \\ \sigma_1, \sigma_2 &\stackrel{\text{i.i.d.}}{\sim} \text{InverseGamma}(1, 1), \\ p(\beta) &\propto 1, \end{aligned} \tag{9}$$

where i.i.d refers to independent and identically distributed. Meanwhile, the Bayesian modal linear regression associated with the DTP-Student- t likelihood (5) is specified by

$$\begin{aligned} Y_i | \mathbf{X}_i, \beta, \sigma_1, \sigma_2, \delta_1, \delta_2 &\sim \text{DTP-Student-}t \left(\mathbf{X}_i^\top \beta, \sigma_1, \sigma_2, \delta_1, \delta_2 \right), \\ \sigma_1, \sigma_2, \delta_1, \delta_2 &\stackrel{\text{i.i.d.}}{\sim} \text{InverseGamma}(1, 1), \\ p(\beta) &\propto 1. \end{aligned} \tag{10}$$

Recall that the weight parameter w of a DTP distribution is fully defined by its scale and shape parameters, so in this case, there is no need to choose a prior for w . Finally, the Bayesian modal linear regression associated with the TPSC-Student- t likelihood (7) is defined as

$$\begin{aligned} Y_i | \mathbf{X}_i, w, \beta, \sigma, \delta &\sim \text{TPSC-Student-}t \left(w, \mathbf{X}_i^\top \beta, \sigma, \delta \right), \\ w &\sim \text{Uniform}(0, 1), \\ \sigma, \delta &\stackrel{\text{i.i.d.}}{\sim} \text{InverseGamma}(1, 1), \\ p(\beta) &\propto 1. \end{aligned} \tag{11}$$

According to Lemma A.2 in the Appendix, all of the proposed Bayesian modal regression models (9) - (11) above have proper posterior distributions. Practitioners can construct various other Bayesian modal regression models using the same strategy shown above. In this paper, we concentrate on the modal regression models based on the FG, DTP-Student- t and TPSC-Student- t likelihoods for the sake of concreteness.

4.2 Uncertainty quantification and model selection

Letting $\Omega = [w, \beta, \sigma_1, \sigma_2]^\top$, the posterior predictive distribution under our Bayesian modal regression model is defined as

$$\begin{aligned} p(Y_{\text{new}} | \mathbf{Y}, \mathbf{X}) &= \int_{\Theta} p(Y_{\text{new}} | \Omega, \mathbf{Y}, \mathbf{X}) p(\Omega | \mathbf{Y}, \mathbf{X}) d\Omega \\ &= \int_{\Theta} p(Y_{\text{new}} | \Omega, \mathbf{X}) p(\Omega | \mathbf{Y}, \mathbf{X}) d\Omega, \end{aligned} \tag{12}$$

where Θ denotes the parameter space, and the last line holds because of the conditional independence of Y_{new} and \mathbf{Y} . Obtaining an approximation of the posterior predictive (12) is computationally inexpensive. With the random number generation algorithm outlined in Section 3 for the GUD family, one can easily draw samples from $p(Y_{\text{new}} | \Omega, \mathbf{X})$

during each iteration in our MCMC algorithm, and then obtain samples from the posterior predictive distribution $p(Y_{\text{new}} | \mathbf{Y}, \mathbf{X})$. In this paper, we use the `hdi` function in the R package `HDInterval` [R Core Team, 2022, Meredith et al., 2018], whose inputs are random samples generated from the posterior predictive distributions, to calculate the highest density intervals (HDI) with a pre-specified nominal level of coverage probability. We use 90% HDI intervals as the posterior prediction intervals for all mean/median/modal regression models that we consider in Sections 2.2, 5, and 6.

Due to the inherent nature of the conditional mode [Yao and Li, 2014], the HDI prediction intervals from modal regression models will usually be *narrower* than those constructed under mean or median regression models, while having the *same* amount of coverage. From a statistical inference point of view, this is a very attractive property of our Bayesian modal regression models – we can obtain high coverage with tighter intervals. Prediction intervals from mean or median regression can sometimes be very conservative and contain many implausible values. We illustrate the benefits of more efficient inference from modal regression in Sections 5 and 6.

As mentioned in Section 4, there are many different GUD likelihoods that a practitioner can choose from in order to conduct Bayesian inference for modal regression. We propose to use the Bayesian leave-one-out expected log posterior density as a model selection criterion for selecting the “best” GUD likelihood to use. The Bayesian leave-one-out expected log predictive density is defined as

$$\text{elpd}_{\text{loo}} = \sum_{i=1}^n \log p(Y_i | Y_{-i}), \quad (13)$$

where Y_{-i} represents all observations except the i -th observation. In (13), “elpd” stands for the theoretical expected log predictive density. Intuitively, if a model fits the data well, its predicted value of Y_i given Y_{-i} should be close to the observed Y_i and $p(Y_i | Y_{-i})$ should be large, for all $i = 1, \dots, n$. Therefore, an adequate model tends to yield a high elpd_{loo} .

We apply the Pareto-smoothed importance sampling method (PSIS) of Vehtari et al. [2017] to obtain an estimate of elpd_{loo} , denoted as $\widehat{\text{elpd}}_{\text{loo}}$. The PSIS estimation of elpd_{loo} has been implemented in an R package `loo`, which is compatible with the Stan programming language [Carpenter et al., 2017]. We used the Stan programming language interfaced with R to implement all regression analysis in this paper. When fitting multiple competing models to the same dataset, the model with the highest $\widehat{\text{elpd}}_{\text{loo}}$ is preferred. For ease of notation, we use the acronym ELPD to replace $\widehat{\text{elpd}}_{\text{loo}}$ in this paper.

5 Simulation studies

We now present a few simulation studies which show that our Bayesian modal regression model is an excellent choice for modeling data that is heavily skewed. Under our simulation settings, simulated data was either left-skewed or right-skewed; and, in addition to the pronounced global conditional mode, there was also a small local mode. We compared our Bayesian modal regression models to Bayesian mean and median regression models. The Bayesian mean regression used a normal likelihood, i.e., for $i = 1, \dots, n$,

$$\begin{aligned} Y_i | \beta, \sigma, \mathbf{X}_i &\sim \mathcal{N}(\mathbf{X}_i^\top \beta, \sigma), \\ \sigma &\sim \text{InverseGamma}(1, 1), \\ p(\beta) &\propto 1. \end{aligned} \quad (14)$$

In line with the literature on parametric Bayesian quantile regression [Yu and Moyeed, 2001, Yu and Zhang, 2005], we also implemented Bayesian median regression using the asymmetric Laplace distribution (ALD), with quantile parameter $p = 0.5$. That is, for $i = 1, \dots, n$, our Bayesian modal median regression model was

$$\begin{aligned} Y_i | \beta, \sigma, \mathbf{X}_i &\sim \text{ALD}(\mathbf{X}_i^\top \beta, \sigma, p = 0.5), \\ \sigma &\sim \text{InverseGamma}(5, 5), \\ p(\beta) &\propto 1. \end{aligned} \quad (15)$$

We stress that in our simulation studies, *none* of the likelihoods used for mean/median/modal regression was exactly the same as the data generating mechanism. Therefore, all considered regression models are “wrong,” creating particularly realistic yet challenging scenarios under which we could more fairly compare the performance across these competing methods.

Table 2: Comparison of Bayesian mean, median, and modal regression models fitted to left-skewed data. Results were averaged across 300 Monte-Carlo replicates of left-skewed datasets. The empirical standard error associated with each Monte-Carlo average is provided in parenthesis following the average.

Likelihood (regression model)	Coverage Rate (%)	Width	ELPD
Normal (mean regression)	93.50 (0.19)	32.25 (1.08)	-104.76 (2.00)
ALD (median regression)	94.69 (0.22)	14.70 (0.49)	-84.81 (1.39)
TPSC-Student- t (modal regression)	94.70 (0.22)	8.36 (0.21)	-59.93 (0.64)

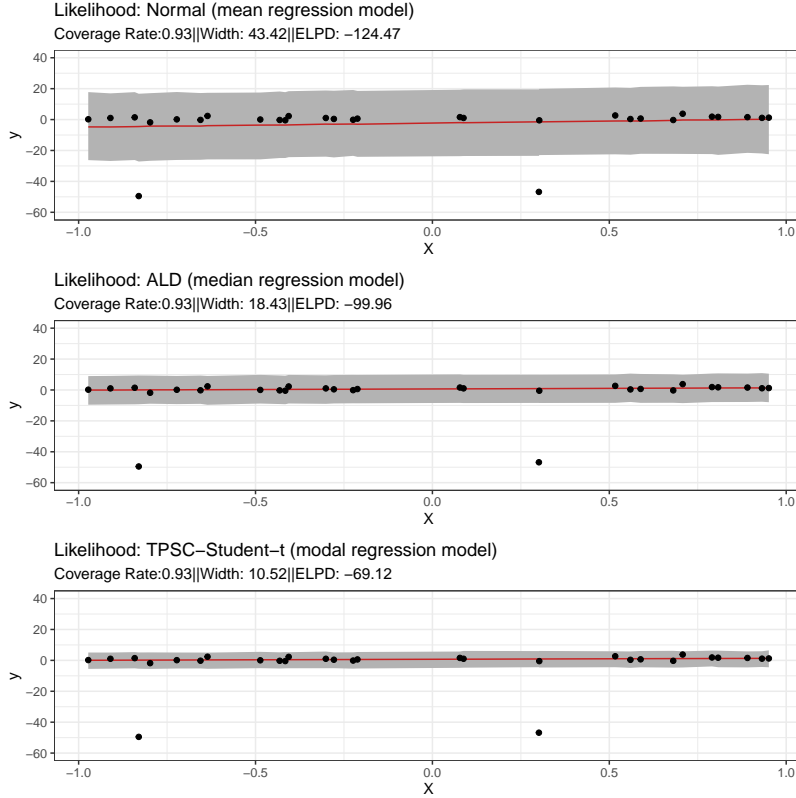


Figure 5: The gray shaded areas show the 90% posterior prediction intervals for the simulated left-skewed data. The solid red line is the estimated median from the posterior predictive distribution. The prediction intervals are narrower for Bayesian modal regression.

5.1 Left-skewed data

We generated $n = 30$ observations from the model,

$$Y_i = \beta_0 + \beta_1 X_i + \epsilon_i,$$

where $\beta_0 = \beta_1 = 1$, $\epsilon_i \stackrel{\text{i.i.d.}}{\sim} 0.05\mathcal{N}(-50, 1^2) + 0.95\mathcal{N}(0, 1^2)$, and X_1, \dots, X_{30} were generated independently from $\text{Uniform}(0, 1)$. We then fit the mean/median/modal regression models to the simulated data. For modal regression, we fit the FG model (9), the DTP-Student- t model (10), and the TPSC-Student- t model (11). Among the modal regression models, we found that the TPSC-Student- t model had the highest ELPD. For the sake of brevity, we present only the results from the models fit with the normal, ALD and TPSC-Student- t likelihoods.

In Figure 5, we provide the empirical coverage rate and the average width of the posterior prediction intervals across $n = 30$ observations under each of mean/median/modal regression model. With the narrowest prediction interval for the same amount of coverage, results from the modal regression model clearly stand out in Figure 5. In addition, the modal regression model with the TPSC-Student- t likelihood had the largest ELPD. Therefore, it was the most appropriate model for the simulated data among the three candidate models in this replication. We repeated this experiment 300 times. Table 2 shows the mean coverage rate, prediction interval width, and ELPD across the 300

Table 3: Comparison of Bayesian mean, median, and modal regression models fitted to right-skewed data. Results were averaged across 300 Monte-Carlo replicates of right-skewed datasets. The empirical standard error associated with each Monte-Carlo average is provided in parenthesis following the average.

Likelihood (regression model)	Coverage Rate (%)	Width	ELPD
Normal (mean regression)	93.67 (0.18)	26.14 (0.95)	-99.41 (1.90)
ALD (median regression)	94.71 (0.22)	12.42 (0.40)	-79.25 (1.29)
TPSC-Student- t (modal regression)	94.73 (0.22)	8.20 (0.20)	-60.04 (0.65)

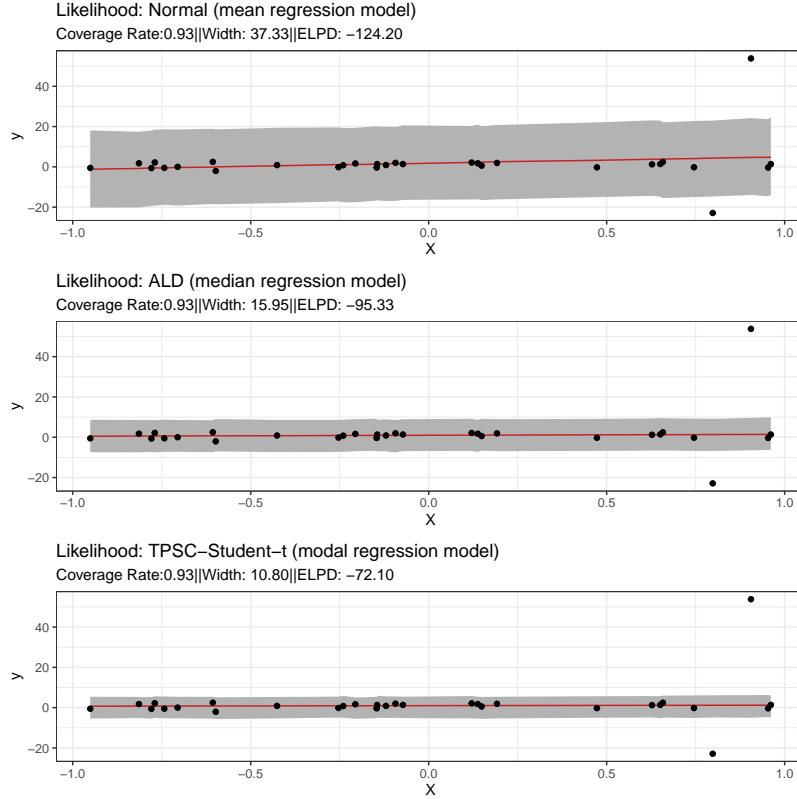


Figure 6: The gray shaded areas show the 90% posterior prediction intervals for the simulated right-skewed data. The solid red line is the estimated median from the posterior predictive distribution. The prediction intervals are narrower for Bayesian modal regression.

replications. The mean regression model with the normal likelihood had the lowest average coverage rate and the widest posterior prediction intervals. Both the median and modal regression models had almost identical average coverage rate. However, the modal regression model had, on average, the narrowest prediction intervals. Since the modal regression model with the TPSC-Student- t likelihood had the largest average ELPD, we conclude that the modal regression model based on the TPSC-Student- t provided the best model fit.

5.2 Right-skewed data

In Section 5.1, we demonstrated the advantages of Bayesian modal regression models when the data was left-skewed. In this section, we investigate our model’s ability to detect right-skewness. We followed the same simulation settings as those in Section 5.1, except the residual error was $\epsilon_i \stackrel{\text{i.i.d.}}{\sim} 0.025\mathcal{N}(-25, 1^2) + 0.95\mathcal{N}(0, 1^2) + 0.025\mathcal{N}(50, 1^2)$ so that the simulated data was right-skewed. We fit the mean/median/modal regression models to this simulated data.

Figure 6 shows that all three models achieved a coverage rate of 93% in one experiment. However, the modal regression model with the TPSC-Student- t likelihood (7) had the narrowest posterior prediction interval and the largest ELPD. Table 3 shows our results averaged across 300 repeated experiments. The modal regression model with the TPSC-

Student- t likelihood had the highest average coverage rate, the narrowest posterior prediction intervals on average, and the largest average ELPD. Therefore, we conclude that the Bayesian modal regression model had the best performance in this right-skewed simulation study.

6 More data applications of Bayesian modal regression

6.1 Uncertainty quantification of air pollution

Inhalable particulate matter referred to as PM10 is any inhalable particle with a diameter of 10 micrometers and smaller. PM10 includes smoke, dust, and metals. In the environmental science literature, it has been found that low (resp. high) wind speeds are associated with high (resp. low) PM10 values [Cichowicz et al., 2020]. In addition, many studies have found that PM10 is associated with heart disease, respiratory disease, and premature death [Schwartz, 1999, Zhao et al., 2017]. We analyzed the PM10 dataset from <http://lib.stat.cmu.edu/datasets/>. This dataset consists of air pollution information collected by the Norwegian Public Roads Administration at Alnabru in Oslo, Norway from October 2001 and August 2003. The response variable is the hourly measurements of the concentration of PM10, while the predictor is the hourly wind speed in meters per second. We fit the following mean/median/modal regression models to this dataset:

$$\mathbb{M}(Y \mid \beta) = \beta_0 + \beta_1 \times \text{windspeed}.$$

Table 4 presents the parameter estimation results of three models. The mean regression model implies that the association between the PM10 concentration and the wind speed is not significant (CI of $(-2.64, 0.12)$). On the other hand, both the median and modal regression models capture the negative association between the PM10 concentration and the wind speed (CIs of $(-2.77, -1.03)$ and $(-1.53, -0.54)$, respectively).

Although both median and modal regression detected the negative association between wind speed and PM10 concentration, we see from Figure 7 that the 90% prediction intervals for median regression (and mean regression) contain many negative values. As the minimum possible measure of PM10 concentration is zero, it is difficult to justify posterior prediction intervals for PM10 that contain many negative values. On the other hand, the 90% prediction intervals from the modal regression model only contain a tiny portion of negative values at very high wind speeds. This suggests that uncertainty quantification under Bayesian modal regression is more reliable in this particular example.

6.2 Detecting a quadratic relationship in serum data

Isaacs et al. [1983] analyzed the relationship between serum concentration (grams per litre) of immunoglobulin-G (IgG) in 298 children aged from 6 months to 6 years. IgG is an antibody that plays an important role in humoral and protective immunity [van de Bovenkamp et al., 2016]. There are ethical difficulties in taking repeated blood samples from healthy subjects. Therefore, researchers often use age as a proxy for determining the reference ranges for IgG in childhood. Previously, Yu and Moyeed [2001] analyzed serum data and modeled IgG concentration with a quadratic model in age. In the spirit of Yu and Moyeed [2001], we fit the following mean/median/modal regression models to this dataset:

$$\mathbb{M}(Y \mid \beta) = \beta_0 + \beta_1 \times \text{Age} + \beta_2 \times \text{Age}^2.$$

Table 5 shows the parameter estimates from the models that we fit to this data. Based on the CIs for β_2 , we see that only the modal regression model is able to detect the quadratic term (CI of $(-0.18, -0.03)$ for modal regression). This finding is somewhat consistent with Royston and Altman [1994] who concluded that a simple linear regression model

Table 4: Parameter estimates obtained from the mean/median/modal regression models fitted to the air pollution data. The mean, 5% quantile, and 95% quantile of the posterior distribution of each regression coefficient are listed under Mean, q5, and q95, respectively.

Likelihood (regression model)	Parameter	Mean	q5	q95
Normal (mean regression)	β_0 (intercept)	41.94	36.80	47.10
	β_1 (windspeed)	-1.27	-2.64	0.12
ALD (median regression)	β_0 (intercept)	32.75	29.50	36.23
	β_1 (windspeed)	-1.87	-2.77	-1.03
TPSC-Student- t (modal regression)	β_0 (intercept)	9.67	7.47	11.75
	β_1 (windspeed)	-1.01	-1.53	-0.54

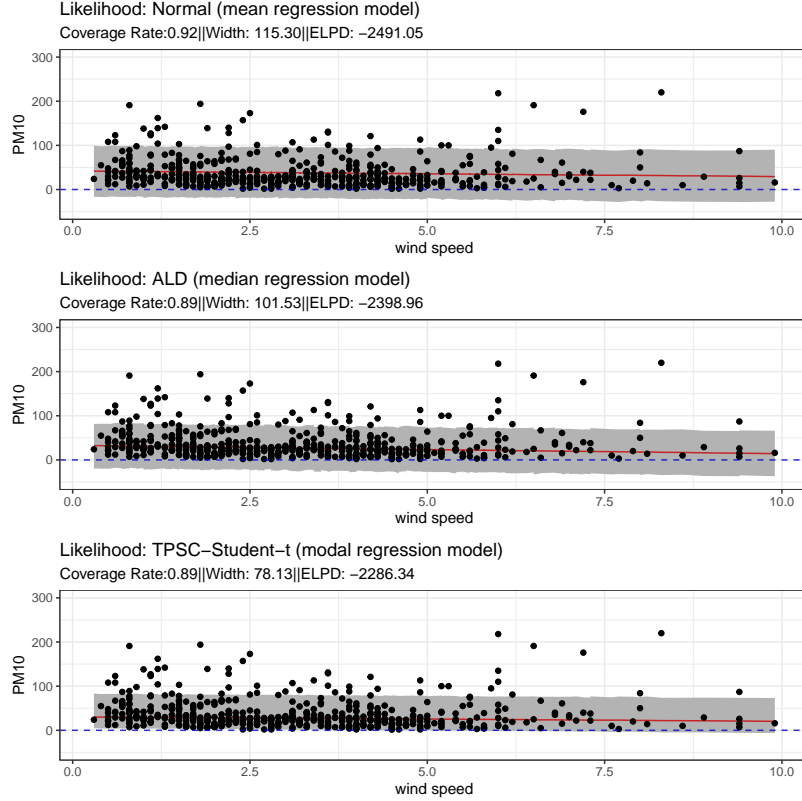


Figure 7: The shaded regions show the 90% posterior prediction intervals for the air pollution data. The blue dashed line is the reference line as the minimum possible value of PM10 (zero). The solid red line represents the estimated median from the posterior predictive distribution.

was inadequate for this same dataset. [Isaacs et al. \[1983\]](#) also suggested that there was a quadratic relationship between the square root of IgG concentration and children’s age.

Table 5 shows that the ELPD of the modal regression model based on the FG likelihood (9) is larger than the ELPD for both the mean or median regression models. In this example, the modal regression model not only provides a different viewpoint (i.e. that there exists a significant quadratic relationship between IgG and age), but it also fits the dataset better according to our model selection criterion.

7 Discussion

In this paper, we have introduced a unifying Bayesian modal regression framework. Namely, we proposed a simple and flexible unimodal distribution family called the GUD family that is suitable for Bayesian modal regression. All members of the GUD family have a location parameter that is also the mode. Members of this family can be either symmetric or asymmetric, either thin-tailed or heavy-tailed, depending on values of the shape and scale parameters.

Compared to mean and quantile regression, work on Bayesian modal regression analysis is quite scarce. Our paper aims to promote Bayesian modal regression as a complement to these other analyses. We demonstrated that our modeling framework based on the GUD family is very versatile and has wide applications in many fields such as economics (the bank deposit data in Section 2.1), criminology (the murder rate data in Section 2.2), environmental science (the air pollution data in Section 6.1), and molecular biology (the serum data in Section 6.2). In particular, we showed that Bayesian modal regression can reveal structures and detect potentially significant covariate effects that are missed by other Bayesian regression models.

To conduct Bayesian inference of the conditional mode, we provided prior elicitation procedures, along with the sufficient conditions under which a flat prior $p(\beta)$ on the regression coefficients β can be used. We proposed a method for constructing posterior prediction intervals and a model selection criterion based on the posterior predictive distribution. We demonstrated that our modal regression models provide very tight prediction intervals with high

Table 5: Parameter estimates from the mean/median/modal regression models fitted to the serum data. The mean, 5% quantile, and 95% quantile of the posterior distribution of each regression coefficient are listed under Mean, q5, and q95, respectively.

Likelihood (regression model)	ELPD	Parameter	Mean	q5	q95
Normal (mean regression)	-627.13	β_0 (intercept)	3.08	2.45	3.72
		β_1 (Age)	0.97	0.45	1.49
		β_2 (Age ²)	-0.05	-0.13	0.04
ALD (median regression)	-638.16	β_0 (intercept)	2.82	2.12	3.57
		β_1 (Age)	1.12	0.53	1.68
		β_2 (Age ²)	-0.07	-0.16	0.03
FG (modal regression)	-623.15	β_0 (intercept)	2.37	1.84	2.89
		β_1 (Age)	1.16	0.72	1.59
		β_2 (Age ²)	-0.11	-0.18	-0.03

coverage, are robust to outliers, and have excellent interpretability. Our modal regression model framework is an especially appealing choice when the data is skewed and/or contains (extreme) outliers.

The modal regression models in this paper contain parametric assumptions, both about the data likelihood and the linear relationship between the covariates and the conditional mode. Instead of using the fully parametric models presented in this manuscript, one may prefer to use Bayesian semiparametric modal regression models instead. A Bayesian semiparametric modal regression model can be constructed either by modeling the conditional mode with a Gaussian process (i.e. we can relax the linearity assumption) and/or by replacing the GUD likelihood with a carefully constructed infinite mixture model that is indexed by the mode (i.e. we can relax the assumption of a known residual error distribution). These exciting extensions to Bayesian modal regression are the topics of ongoing work.

Acknowledgments

The last author was generously supported by NSF grant DMS-2015528.

Appendices

A Sufficient conditions for posterior propriety

Since we used an improper prior, $p(\beta) \propto 1$, for the regression coefficients β in our Bayesian modal regression models, it is important to check that the posterior distribution is proper. Theorem A.1 gives sufficient conditions under which the GUD likelihood (1) and suitably chosen priors on the model parameters lead to a proper posterior. Lemma A.2 extends this result to the regression setting. We stress that our results are *nonasymptotic*; that is, for any fixed sample size n and fixed number of covariates p , the posterior is proper under very mild conditions.

Theorem A.1. *Assume that the following conditions are satisfied:*

- (A) *Both ranges of $f_1(\cdot \mid \theta, \sigma_1)$ and $f_2(\cdot \mid \theta, \sigma_2)$ are bounded from above for any given θ , σ_1 and σ_2 .*
- (B) *Both $f_1(\cdot \mid \theta, \sigma_1)$ and $f_2(\cdot \mid \theta, \sigma_2)$ have proper posterior distributions under the flat prior $p(\theta) \propto 1$. That is, $\int_{-\infty}^{+\infty} f_1(\cdot \mid \theta, \sigma_1) d\theta < +\infty$ and $\int_{-\infty}^{+\infty} f_2(\cdot \mid \theta, \sigma_2) d\theta < +\infty$.*
- (C) *The priors for w , σ_1 and σ_2 are all proper.*

Then the posterior distribution $p(w, \theta, \sigma_1, \sigma_2 \mid Y_1, \dots, Y_n)$, under a GUD likelihood (1) and a flat prior $p(\theta) \propto 1$ on the location parameter θ is proper.

Proof. By assumption (A), there exists a constant $c > 0$ such that

$$\prod_{i=1}^n f(y_i | w, \theta, \sigma_1, \sigma_2) \leq c \times f(y_1 | w, \theta, \sigma_1, \sigma_2).$$

Applying Bayes' theorem, we have

$$\begin{aligned} p(w, \theta, \sigma_1, \sigma_2 | Y_1, \dots, Y_n) &\propto \left\{ \prod_{i=1}^n f(y_i | w, \theta, \sigma_1, \sigma_2) \right\} p(w) p(\theta) p(\sigma_1) p(\sigma_2) \\ &\leq c \{w f_1(y_1 | \theta, \sigma_1) + (1-w) f_2(y_1 | \theta, \sigma_2)\} p(w) p(\theta) p(\sigma_1) p(\sigma_2). \end{aligned}$$

By assumption (B),

$$\int_{-\infty}^{+\infty} \{w f_1(y_1 | \theta, \sigma_1) + (1-w) f_2(y_1 | \theta, \sigma_2)\} p(\theta) d\theta < +\infty.$$

By assumption (C), the priors for w, σ_1 and σ_2 are all proper, and so the posterior $p(w, \theta, \sigma_1, \sigma_2 | Y_1, \dots, Y_n)$ is proper. \square

Condition (A) is very mild and indicated by restriction (R1) stated in Section 3 since, for $k = 1, 2$, $f_k(\cdot | \theta, \sigma_k) \leq f_k(\theta | \theta, \sigma_k)$, which is finite as implied by the existence of a well-defined mode θ for each component distribution in the mixture. Condition (B) can be checked easily. For example, if $f_2(y | \theta, \sigma_2) = f_{\text{Gumbel}}(y | \theta, \sigma_2)$, one can show that $\int_{-\infty}^{+\infty} f_{\text{Gumbel}}(y | \theta, \sigma_2) d\theta = \sigma_2 < +\infty$.

We now extend the result in Theorem A.1 to the regression setting. Lemma A.2 enables us to use the noninformative flat prior $p(\beta) \propto 1$ for the regression coefficients β in Bayesian modal regression.

Lemma A.2. *For independent observations $(\mathbf{X}_1, Y_1), \dots, (\mathbf{X}_n, Y_n)$, suppose that $\max_{1 \leq i \leq n} |\mathbf{X}_i^\top \beta| < +\infty$ and that the following assumptions hold:*

- (D) *For any $i = 1, \dots, n$, both ranges of $f_1(\cdot | \mathbf{X}_i^\top \beta, \sigma_1)$ and $f_2(\cdot | \mathbf{X}_i^\top \beta, \sigma_2)$ are bounded from above for any given $\mathbf{X}_i^\top \beta, \sigma_1$ and σ_2 .*
- (E) *For any $i = 1, \dots, n$, both $f_1(\cdot | \mathbf{X}_i^\top \beta, \sigma_1)$ and $f_2(\cdot | \mathbf{X}_i^\top \beta, \sigma_2)$ have proper posterior distributions under the flat prior $p(\beta) \propto 1$. That is $\int_{\mathbb{R}^p} f_1(\cdot | \mathbf{X}_i^\top \beta, \sigma_1) d\beta < +\infty$ and $\int_{\mathbb{R}^p} f_2(\cdot | \mathbf{X}_i^\top \beta, \sigma_2) d\beta < +\infty$.*
- (F) *The priors for w, σ_1 , and σ_2 are proper.*

Then the posterior distribution $p(w, \beta, \sigma_1, \sigma_2 | \mathbf{X}, \mathbf{Y})$ under the GUD likelihood (1) and a flat prior $p(\beta) \propto 1$ on β is proper.

Proof. By assumption (D), there must exist a constant $c > 0$ such that

$$\prod_{i=1}^n f(Y_i | w, \mathbf{X}_i^\top \beta, \sigma_1, \sigma_2) \leq c \times f(Y_1 | w, \mathbf{X}_1^\top \beta, \sigma_1, \sigma_2),$$

where $f(Y_1 | w, \mathbf{X}_1^\top \beta, \sigma_1, \sigma_2)$ is the pdf function defined in (1). Applying Bayes' theorem, we have

$$\begin{aligned} p(w, \beta, \sigma_1, \sigma_2 | Y_1, \dots, Y_n) &\propto \left\{ \prod_{i=1}^n f(Y_i | w, \mathbf{X}_i^\top \beta, \sigma_1, \sigma_2) \right\} p(w) p(\beta) p(\sigma_1) p(\sigma_2) \\ &\leq c \{w f_1(Y_1 | \mathbf{X}_1^\top \beta, \sigma_1) + (1-w) f_2(Y_1 | \mathbf{X}_1^\top \beta, \sigma_2)\} p(w) p(\beta) p(\sigma_1) p(\sigma_2). \end{aligned}$$

Further, by assumption (E),

$$\int_{\mathbb{R}^p} \{w f_1(Y_1 | \mathbf{X}_1^\top \beta, \sigma_1) + (1-w) f_2(Y_1 | \mathbf{X}_1^\top \beta, \sigma_2)\} p(\beta) d\beta < +\infty.$$

Since the priors for w, σ_1 and σ_2 are all proper by assumption (F), the posterior distribution $p(w, \beta, \sigma_1, \sigma_2 | \mathbf{X}, \mathbf{Y})$ is also proper. \square

B The Lognormal Mixture Distribution

To demonstrate how researchers can add new members to the GUD family, we present the construction of the lognormal mixture distribution (logNM) below. Here, we pick the lognormal distribution because the lognormal distribution is right-skewed and unimodal. We construct a location-shift lognormal distribution such that the transformed lognormal distribution is still right-skewed but has a mode at 0. Next, we flip the location-shift lognormal distribution at 0 to get a left-skewed unimodal lognormal distribution. Finally, we mix the left- and right-skewed lognormal distribution together to construct the logNM distribution. More details of the construction of logNM can be found in (16)-(17).

The pdf of the lognormal distribution is

$$f_{\log N}(y | \mu, \nu) = \frac{1}{y\nu\sqrt{2\pi}} \exp\left(-\frac{(\ln(y) - \mu)^2}{2\nu^2}\right) \mathbb{I}(y > 0), \quad (16)$$

where $\mu \in (-\infty, +\infty)$ and $\nu > 0$ are two parameters, and the mode is given by $\exp(\mu - \nu^2)$. We define the pdf of logNM as a mixture of two lognormal pdfs formulated as follows,

$$\begin{aligned} f_{\log NM}(y | w, \theta, \sigma_1, \sigma_2) &= wf_1(y|\theta, \sigma_1) + (1-w)f_2(y|\theta, \sigma_2), \\ f_1(y|\theta, \sigma_1) &= f_{\log N}(\exp(\mu_1 - \nu_1^2) - (y - \theta) | \mu_1, \nu_1), \\ f_2(y|\theta, \sigma_2) &= f_{\log N}(\exp(\mu_2 - \nu_2^2) + (y - \theta) | \mu_2, \nu_2), \end{aligned} \quad (17)$$

where $\sigma_1 = [\mu_1, \nu_1]^\top$ and $\sigma_2 = [\mu_2, \nu_2]^\top$. It can be shown that both component distributions in (17) are unimodal at θ , with continuous densities over the real line, one left-skewed and the other right-skewed. Moreover, the pdfs of the individual lognormal mixture components in (17) have 0 at the right and left boundaries of their supports. Hence, the pdf of the logNM distribution is continuous in all of \mathbb{R} . Having verified that all three restrictions (R1)-(R3) for the GUD family (introduced in Section 3 of the main manuscript), we can proceed to use the logNM likelihood (18) for Bayesian modal regression.

Figure 8 demonstrates that the logNM distributions can be asymmetric or symmetric given different combinations of parameter values. The top panel shows that, with an increase of μ_2 , the right tail of the logNM distribution becomes heavier while its left tail remains almost the same. The bottom panel shows how ν_1 influences the amount of skewness of the logNM distribution when all three logNM distributions are left-skewed.

Practitioners can build a Bayesian modal linear regression model based on the logNM likelihood (18) as follows:

$$\begin{aligned} Y_i | \mathbf{X}_i, w, \beta, \sigma_1, \sigma_2 &\stackrel{\text{ind}}{\sim} \log NM\left(w, \mathbf{X}_i^\top \beta, \mu_1, \nu_1, \mu_2, \nu_2\right), \\ w &\sim \text{Uniform}(0, 1), \\ \nu_1, \nu_2 &\stackrel{\text{i.i.d}}{\sim} \text{InverseGamma}(1, 1), \\ \mu_1, \mu_2 &\stackrel{\text{i.i.d}}{\sim} \mathcal{N}(0, 100^2), \\ p(\beta) &\propto \mathcal{N}_p(\mathbf{0}, 10^2 \times \mathbf{I}_{p \times p}), \end{aligned} \quad (18)$$

where $\mathbf{I}_{p \times p}$ stands for the p by p identity matrix and β is a p -dimension random vector. If one wishes to use the flat prior $p(\beta) \propto 1$, then it is necessary to check conditions (E), (F) and (G) of Lemma A.2 in the main article.

If researchers have another right-skewed or a left-skewed distribution to work with, then they can mimic the construction of the logNM above to propose a member of the GUD family that works for their applications. For example, one can use the reparameterized unimodal right-skewed Gamma distribution from Bourguignon et al. [2020] to construct a new type I GUD and a corresponding modal regression model.

In the following lemma, we show why flat priors *cannot* be used for μ_1 and(or) μ_2 in the Bayesian modal regression model based on the logNM distribution. This simple example demonstrates why we should *avoid* placing improper priors on the *non*-location parameters in Bayesian modal regression models based on the GUD family.

Lemma B.1. *Endowing μ_1 and(or) μ_2 with flat priors $p(\mu_1) \propto 1$ and(or) $p(\mu_2) \propto 1$ leads to an improper posterior distribution under the logNM model (18).*

Proof. We want to show that

$$\int_{-\infty}^{+\infty} \prod_{i=1}^n f_{\log NM}(y_i | w, \theta, \sigma_1, \sigma_2, \mu_1, \mu_2) d\mu_1 = +\infty,$$

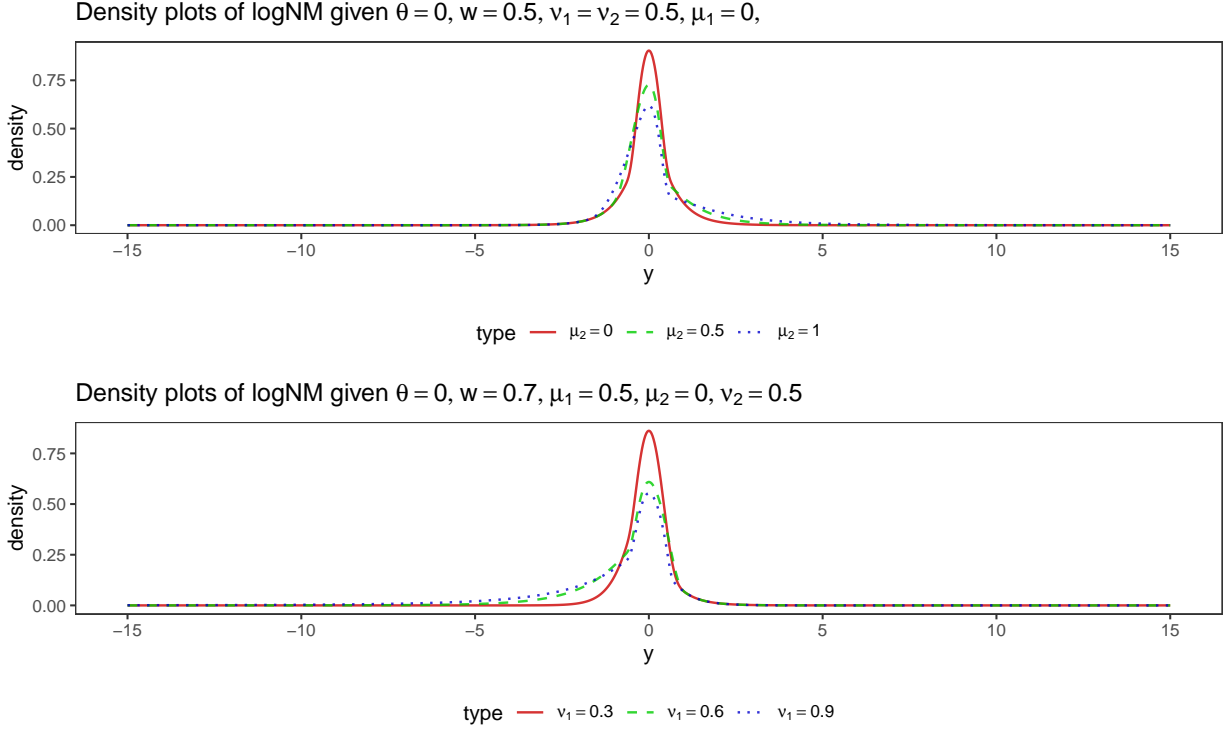


Figure 8: Density plots of the logNM distribution given different combinations of parameter values.

and(or),

$$\int_{-\infty}^{+\infty} \prod_{i=1}^n f_{\log\text{NM}}(y_i | w, \theta, \sigma_1, \sigma_2, \mu_1, \mu_2) d\mu_2 = +\infty.$$

Since

$$f_{\log\text{NM}}(y | w, \theta, \sigma_1, \sigma_2, \mu_1, \mu_2) = w f_{\log\text{N}}(\exp(\mu_1 - \nu_1^2) - (y - \theta) | \theta, \mu_1, \nu_1) + (1 - w) f_{\log\text{N}}(\exp(\mu_2 - \nu_2^2) + (y - \theta) | \theta, \mu_2, \nu_2),$$

and any pdf must be nonnegative, it suffices to show that

$$\int_{-\infty}^{+\infty} f_{\log\text{N}}(\exp(\mu_1 - \nu_1^2) - (y - \theta) | \theta, \mu_1, \nu_1) d\mu_2 = \infty,$$

and(or)

$$\int_{-\infty}^{+\infty} f_{\log\text{N}}(\exp(\mu_2 - \nu_2^2) + (y - \theta) | \theta, \mu_2, \nu_2) d\mu_1 = \infty.$$

Both the integrals above are non-finite. This completes the proof. \square

Following the same arguments as those in Lemma B.1, one can show that improper priors such as $p(\nu_1) \propto 1/\nu_1$ and(or) $p(\nu_2) \propto 1/\nu_2$ will also lead to an improper posterior distribution. A general rule is that, for the Bayesian modal regression models based on the GUD family, using improper prior(s) for any parameter in $(\sigma_1 \cup \sigma_2) \setminus (\sigma_1 \cap \sigma_2)$ leads to an improper posterior distribution. Here, $A \setminus B = A \cap B^c$ denotes a collection of elements in A but not in B .

This result should not be surprising. As pointed out by Diebolt and Robert [1994], improper priors should in general not be used for Bayesian modeling of mixture distributions. We note, however, that the reasoning of Diebolt and Robert [1994] does not necessarily apply to the *location* parameter θ (or the mode). This is because the mode θ is shared by *both* left- and right-skewed components in our proposed GUD family of distributions. Therefore, in the main article, we were able to derive sufficient conditions under which a totally noninformative flat prior $p(\theta) \propto 1$ or $p(\beta) \propto 1$ could still be used to infer the conditional *mode*. On the other hand, we would recommend against using improper priors for any of the *non*-location parameters (i.e. the shape/scale parameters) in Bayesian modal regression based on the GUD family.

C A Short Note About Markov Chain Monte Carlo (MCMC)

Readers who are familiar with Bayesian modeling of mixture distributions may wonder why we do not use the data augmentation “trick” to design a specific MCMC algorithm for modal regression models based on the GUD family. The problem lies in the type II distributions of the GUD family. If $\mathcal{D}_1 \cap \mathcal{D}_2 = \emptyset$, then the latent variable conditional on other parameters and observed data becomes a degenerate random variable. This degenerate random variable will not behave randomly.

To demonstrate that we have a degenerate random variable, let us consider a simple case with a single observation. Recall that the type II GUD has the pdf

$$f(y | w, \theta, \sigma_1, \sigma_2) = w f_1(y | \theta, \sigma_1) I(y < \theta) + (1 - w) f_2(y | \theta, \sigma_2) I(y \geq \theta).$$

Introducing the latent variable z , we have the joint pdf as

$$f(y, z | w, \theta, \sigma_1, \sigma_2) = [w f_1(y | \theta, \sigma_1) I(y < \theta)]^z [(1 - w) f_2(y | \theta, \sigma_2) I(y \geq \theta)]^{1-z}.$$

The conditional distribution of z is then

$$\begin{aligned} p(z | w, \theta, \sigma_1, \sigma_2, y) &\propto f(y, z | w, \theta, \sigma_1, \sigma_2) \\ &\sim \text{Bernoulli} \left(\frac{w f_1(y | \theta, \sigma_1) I(y < \theta)}{w f_1(y | \theta, \sigma_1) I(y < \theta) + (1 - w) f_2(y | \theta, \sigma_2) I(y \geq \theta)} \right). \end{aligned}$$

Similarly, the conditional distribution of θ is

$$p(\theta | w, \sigma_1, \sigma_2, y, z) \propto f(y, z | w, \theta, \sigma_1, \sigma_2) p(\theta).$$

The conditional mean of the latent variable z can only be 0 or 1 since $y < \theta$ and $y \geq \theta$ cannot happen at the same time. Hence, the latent variable becomes a degenerate random variable during the MCMC iterations. Without loss of generality, let us assume $z = 1$ in the first iteration of the MCMC. It is not hard to see that, during the MCMC iterations, the updated values of θ can only be larger than y . This leads to z being equal to 1 for the rest of the iterations in the MCMC algorithm. However, if the true value of θ is smaller than y , then the MCMC chain will never reach the true value. Similarly, if $z = 0$ in the first iteration of the MCMC, then all updated values of θ can only be smaller than y .

In conclusion, for Bayesian modal regression models based on the type II GUD subfamily, the latent variable data augmentation algorithm will *not* explore the *whole* parameter space. Hence, it is *non-ergodic*. As a consequence of this, we do *not* use the data augmentation “trick” for mixture models in our MCMC algorithm. Instead, we use the No-U-Turn Sampler implemented in the STAN software [Hoffman et al., 2014, Carpenter et al., 2017].

D Convergence Diagnostics for the Real Data Applications and Simulation Studies

In this section, we include more details about posterior inference, convergence diagnostics, and traceplots for the four data application examples and two simulation studies from the main manuscript. The `rhat`, which has the theoretical minimum value as 1, is a statistic measuring the convergence of the MCMC chains. To obtain reliable posterior inference, it is recommended that `rhat` should be near 1 or at least less than 1.1 (page 287 of Gelman et al. [2013]). The `ess_bulk` and `ess_tail` are the bulk and tail effective sample size respectively. The `ess_tail` is defined as the minimum of the effective sample sizes for the 5% and 95% quantiles. The recommended lower threshold for `ess_bulk` and `ess_tail` is 400 [Vehtari et al., 2021]. All of the `rhat`, `ess_bulk` and `ess_tail` summary statistics from our analyses in the main manuscript satisfy these recommended thresholds.

All of the traceplots presented in this section also indicate that the MCMC chains mixed well, with no convergence issues. We ran four MCMC chains for each model that was fit and used the combined MCMC samples to approximate the posterior distributions. For the intercept-only regression model fit to the bank deposits data (Section 2.1 of the main manuscript), we set the number of warmup iterations as 10,000 and the number of post-warmup iterations as 20,000 for each chain. For all other models in the main article, we set the number of warmup iterations as 10,000 and the number of post-warmup iterations as 10,000 for each of the four MCMC chains.

D.1 Bank Deposits Application

```
# A tibble: 6 × 10
  variable    mean    median    sd    mad      q5     q95  rhat ess_bulk ess_tail
  <chr>      <dbl>    <dbl> <dbl> <dbl> <dbl> <dbl> <dbl> <dbl> <dbl>
1 lp__      -288.    -288.  1.63  1.43 -291. -286.  1.00  36112.  47263.
```

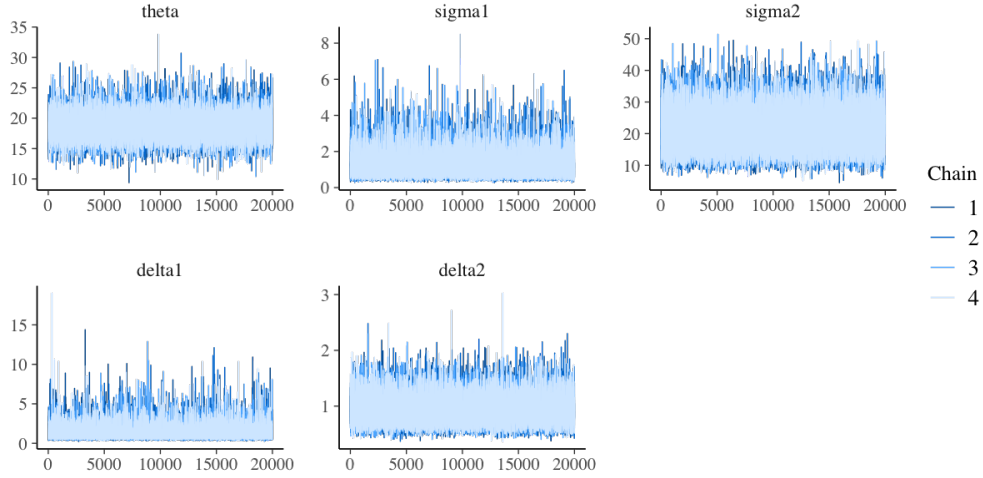


Figure 9: Traceplots for the modal regression model based on the DTP-Student- t likelihood fit to the bank deposits data (Section 2.1 of the main manuscript).

2	sigma1	1.20	1.08	0.559	0.437	0.567	2.25	1.00	51221.	45698.
3	sigma2	20.5	20.0	5.37	5.20	12.6	30.1	1.00	46745.	49890.
4	delta1	1.34	1.16	0.745	0.503	0.597	2.67	1.00	70792.	47613.
5	delta2	0.915	0.888	0.211	0.198	0.621	1.30	1.00	51342.	54038.
6	theta	18.7	18.7	1.80	1.67	15.9	21.6	1.00	42904.	40976.

D.2 Crime Rate Application

mean regression - Normal likelihood

```
# A tibble: 4 × 10
```

	variable	mean	median	sd	mad	q5	q95	rhat	ess_bulk	ess_tail
	<chr>	<dbl>	<dbl>	<dbl>	<dbl>	<dbl>	<dbl>	<dbl>	<dbl>	<dbl>
1	alpha	-24.2	-24.2	5.33	5.28	-33.0	-15.4	1.00	15362.	20037.
2	beta[1]	0.467	0.466	0.163	0.161	0.200	0.738	1.00	17845.	20507.
3	beta[2]	1.14	1.14	0.227	0.225	0.765	1.51	1.00	18553.	22035.
4	beta[3]	0.0677	0.0677	0.0341	0.0340	0.0121	0.124	1.00	23524.	24312.

median regression - ALD likelihood

```
# A tibble: 4 × 10
```

	variable	mean	median	sd	mad	q5	q95	rhat	ess_bulk	ess_tail
	<chr>	<dbl>	<dbl>	<dbl>	<dbl>	<dbl>	<dbl>	<dbl>	<dbl>	<dbl>
1	alpha	-1.34	-1.18	3.39	3.28	-7.16	3.89	1.00	9895.	11638.
2	beta[1]	-0.118	-0.123	0.0964	0.0933	-0.268	0.0471	1.00	10933.	13580.
3	beta[2]	0.437	0.432	0.138	0.128	0.216	0.673	1.00	11652.	13166.
4	beta[3]	0.0555	0.0554	0.0161	0.0158	0.0294	0.0818	1.00	17520.	18274.

modal regression - TPSC-Student- t

```
# A tibble: 4 × 10
```

	variable	mean	median	sd	mad	q5	q95	rhat	ess_bulk	ess_tail
	<chr>	<dbl>	<dbl>	<dbl>	<dbl>	<dbl>	<dbl>	<dbl>	<dbl>	<dbl>
1	alpha	1.12	1.25	2.68	2.62	-3.56	5.29	1.00	13814.	16690.
2	beta[1]	-0.199	-0.204	0.0825	0.0805	-0.327	-0.0552	1.00	14342.	17771.
3	beta[2]	0.243	0.250	0.138	0.144	0.00688	0.459	1.00	10233.	15650.
4	beta[3]	0.0636	0.0624	0.0153	0.0149	0.0403	0.0906	1.00	10145.	9351.

D.3 Air Pollution Application

mean regression - Normal likelihood

```
# A tibble: 2 × 10
  variable mean median sd mad q5 q95 rhat ess_bulk ess_tail
  <chr> <dbl> <dbl> <dbl> <dbl> <dbl> <dbl> <dbl> <dbl> <dbl>
1 alpha 41.9 41.9 3.12 3.14 36.8 47.1 1.00 15822. 19673.
2 beta[1] -1.27 -1.26 0.841 0.849 -2.64 0.116 1.00 15614. 18993.
```

median regression - ALD likelihood

```
# A tibble: 2 × 10
  variable mean median sd mad q5 q95 rhat ess_bulk ess_tail
  <chr> <dbl> <dbl> <dbl> <dbl> <dbl> <dbl> <dbl> <dbl> <dbl>
1 alpha 32.8 32.7 2.05 2.03 29.5 36.2 1.00 13984. 16088.
2 beta[1] -1.87 -1.85 0.530 0.524 -2.77 -1.03 1.00 14043. 15873.
```

modal regression - TPSC-Student-t

```
# A tibble: 2 × 10
  variable mean median sd mad q5 q95 rhat ess_bulk ess_tail
  <chr> <dbl> <dbl> <dbl> <dbl> <dbl> <dbl> <dbl> <dbl> <dbl>
1 alpha 9.67 9.76 1.44 1.18 7.46 11.7 1.00 4268. 1787.
2 beta[1] -1.01 -0.997 0.309 0.302 -1.53 -0.538 1.00 4581. 1832.
```

D.4 Serum Data Application

mean regression - Normal likelihood

```
# A tibble: 3 × 10
  variable mean median sd mad q5 q95 rhat ess_bulk ess_tail
  <chr> <dbl> <dbl> <dbl> <dbl> <dbl> <dbl> <dbl> <dbl> <dbl>
1 alpha 3.08 3.08 0.384 0.380 2.45 3.72 1.00 10706. 15240.
2 beta[1] 0.969 0.969 0.313 0.311 0.451 1.48 1.00 9820. 13370.
3 beta[2] -0.0458 -0.0460 0.0510 0.0508 -0.130 0.0385 1.00 10328. 14088.
```

median regression - ALD likelihood

```
# A tibble: 3 × 10
  variable mean median sd mad q5 q95 rhat ess_bulk ess_tail
  <chr> <dbl> <dbl> <dbl> <dbl> <dbl> <dbl> <dbl> <dbl> <dbl>
1 alpha 2.82 2.81 0.441 0.449 2.12 3.57 1.00 8105. 12034.
2 beta[1] 1.12 1.13 0.348 0.352 0.527 1.68 1.00 7692. 10288.
3 beta[2] -0.0656 -0.0668 0.0574 0.0576 -0.157 0.0314 1.00 8134. 10823.
```

modal regression - TPSC-Student-t

```
# A tibble: 3 × 10
  variable mean median sd mad q5 q95 rhat ess_bulk ess_tail
  <chr> <dbl> <dbl> <dbl> <dbl> <dbl> <dbl> <dbl> <dbl> <dbl>
1 alpha 2.37 2.37 0.320 0.316 1.84 2.89 1.00 12565. 17546.
2 beta[1] 1.15 1.16 0.264 0.264 0.720 1.59 1.00 11055. 16023.
3 beta[2] -0.107 -0.107 0.0441 0.0438 -0.179 -0.0338 1.00 11692. 17288.
```


D.5 Left-Skewed Simulation Study

mean regression - Normal likelihood

```
# A tibble: 2 × 10
  variable mean median sd mad q5 q95 rhat ess_bulk ess_tail
<chr> <dbl> <dbl> <dbl> <dbl> <dbl> <dbl> <dbl> <dbl> <dbl>
1 alpha -2.32 -2.32 2.37 2.33 -6.21 1.59 1.00 36206. 27772.
2 beta[1] 2.64 2.66 3.67 3.59 -3.36 8.66 1.00 34513. 27175.
```

median regression - ALD likelihood

```
# A tibble: 2 × 10
  variable mean median sd mad q5 q95 rhat ess_bulk ess_tail
<chr> <dbl> <dbl> <dbl> <dbl> <dbl> <dbl> <dbl> <dbl> <dbl>
1 alpha 0.653 0.648 0.468 0.445 -0.0964 1.43 1.00 31916. 25876.
2 beta[1] 0.751 0.746 0.755 0.693 -0.483 2.00 1.00 34392. 25226.
```

modal regression - TPSC-Student-t

```
# A tibble: 2 × 10
  variable mean median sd mad q5 q95 rhat ess_bulk ess_tail
<chr> <dbl> <dbl> <dbl> <dbl> <dbl> <dbl> <dbl> <dbl> <dbl>
1 alpha 0.847 0.819 0.386 0.364 0.265 1.52 1.00 20058. 19143.
2 beta[1] 0.639 0.644 0.334 0.321 0.0800 1.18 1.00 29384. 25974.
```

D.6 Right-Skewed Simulation Study

mean regression - Normal likelihood

```
# A tibble: 2 × 10
  variable mean median sd mad q5 q95 rhat ess_bulk ess_tail
<chr> <dbl> <dbl> <dbl> <dbl> <dbl> <dbl> <dbl> <dbl> <dbl>
1 alpha 1.83 1.82 2.01 1.97 -1.46 5.12 1.00 37079. 27813.
2 beta[1] 3.12 3.11 3.43 3.35 -2.51 8.76 1.00 34832. 26126.
```

median regression - ALD likelihood

```
# A tibble: 2 × 10
  variable mean median sd mad q5 q95 rhat ess_bulk ess_tail
<chr> <dbl> <dbl> <dbl> <dbl> <dbl> <dbl> <dbl> <dbl> <dbl>
1 alpha 0.976 0.986 0.470 0.464 0.192 1.73 1.00 30065. 23935.
2 beta[1] 0.473 0.487 0.944 0.925 -1.12 1.98 1.00 28958. 26648.
```

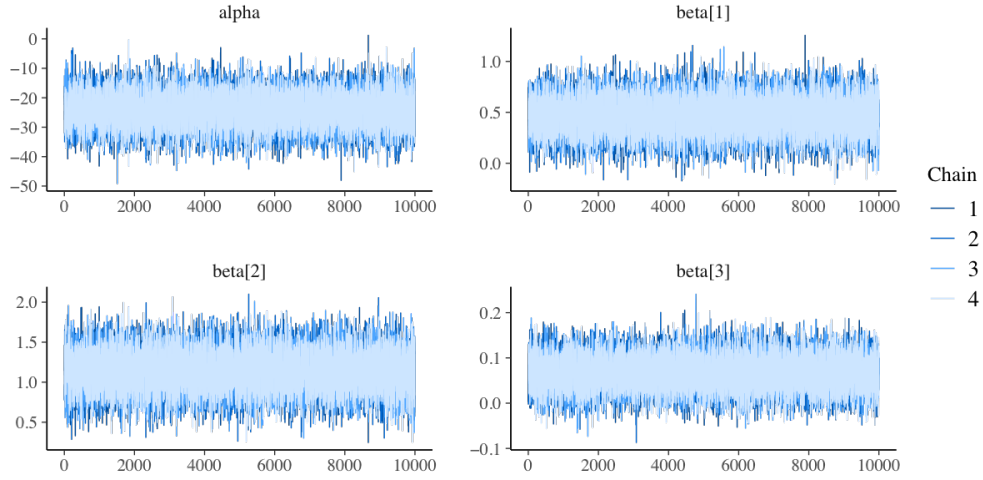
modal regression - TPSC-Student-t

```
# A tibble: 2 × 10
  variable mean median sd mad q5 q95 rhat ess_bulk ess_tail
<chr> <dbl> <dbl> <dbl> <dbl> <dbl> <dbl> <dbl> <dbl> <dbl>
1 alpha 1.33 1.41 0.532 0.517 0.328 2.05 1.00 14412. 15244.
2 beta[1] 0.257 0.211 0.589 0.612 -0.633 1.28 1.00 20263. 24407.
```

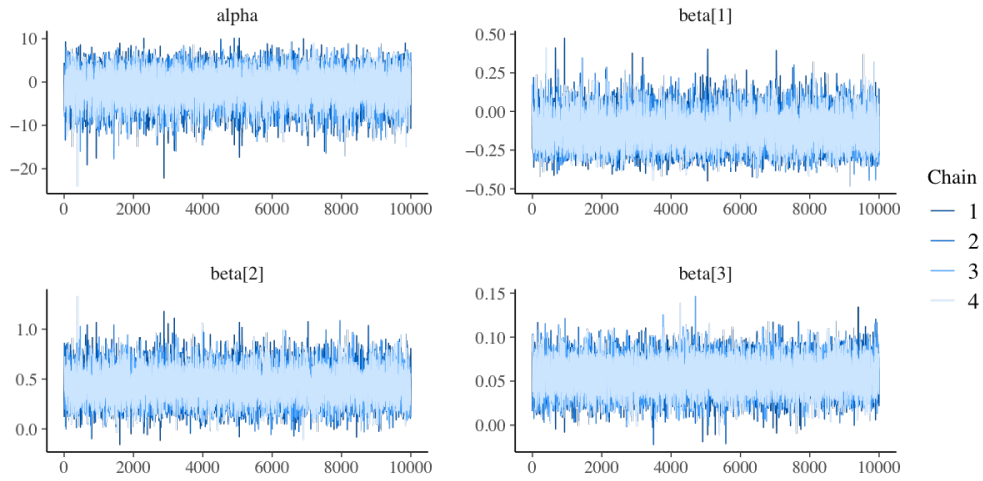
References

- Roger Koenker, Victor Chernozhukov, Xuming He, and Limin Peng. *Handbook of Quantile Regression*. Chapman and Hall/CRC, 2017.
- Thomas W Sager and Ronald A Thisted. Maximum likelihood estimation of isotonic modal regression. *The Annals of Statistics*, pages 690–707, 1982.
- Myoung-jae Lee. Mode regression. *Journal of Econometrics*, 42(3):337–349, 1989.
- Myoung-Jae Lee. Quadratic mode regression. *Journal of Econometrics*, 57(1-3):1–19, 1993.
- Weixin Yao and Longhai Li. A new regression model: Modal linear regression. *Scandinavian Journal of Statistics*, 41(3):656–671, 2014.
- Yen-Chi Chen. Modal regression using kernel density estimation: A review. *Wiley Interdisciplinary Reviews: Computational Statistics*, 10(4):e1431, 2018.
- Katerina Aristodemou. *New regression methods for measures of central tendency*. PhD thesis, 2014.
- Marcelo Bourguignon, Jeremias Leão, and Diego I Gallardo. Parametric modal regression with varying precision. *Biometrical Journal*, 62(1):202–220, 2020.
- Haiming Zhou and Xianzheng Huang. Parametric mode regression for bounded responses. *Biometrical Journal*, 62(7):1791–1809, 2020.
- André FB Menezes, Josmar Mazucheli, and Subrata Chakraborty. A collection of parametric modal regression models for bounded data. *Journal of Biopharmaceutical Statistics*, 31(4):490–506, 2021.
- Keming Yu and Katerina Aristodemou. Bayesian mode regression. *arXiv preprint arXiv:1208.0579*, 2012.
- Haiming Zhou and Xianzheng Huang. Bayesian beta regression for bounded responses with unknown supports. *Computational Statistics & Data Analysis*, 167:107345, 2022.
- Paul Damien, Stephen Walker, et al. Bayesian mode regression using mixtures of triangular densities. *Journal of Econometrics*, 197(2):273–283, 2017.
- Jess Benhabib and Alberto Bisin. Skewed wealth distributions: Theory and empirics. *Journal of Economic Literature*, 56(4):1261–91, 2018.
- Andrew F Siegel. *Practical Business Statistics*. Academic Press, 2016.
- Alan Agresti, Christine Franklin, and Bernhard Klingenberg. *Statistics: The Art and Science of Learning from Data*. Pearson Education, 5 edition, 2021.
- Lance Lochner. Education and crime. In *The Economics of Education*, pages 109–117. Elsevier, 2020.
- Randi Hjalmarsson and Lance Lochner. The impact of education on crime: International evidence. *CESifo DICE Report*, 10(2):49–55, 2012.
- Grzegorz Sitek. The modes of a mixture of two normal distributions. *Silesian Journal of Pure and Applied Mathematics*, 6(1):59–67, 2016.
- Javad Behboodian. On the modes of a mixture of two normal distributions. *Technometrics*, 12(1):131–139, 1970.
- Henry Teicher. Identifiability of finite mixtures. *The Annals of Mathematical Statistics*, pages 1265–1269, 1963.
- Carmen Fernández and Mark FJ Steel. On bayesian modeling of fat tails and skewness. *Journal of the American Statistical Association*, 93(441):359–371, 1998.
- FJ Rubio and MFJ Steel. Bayesian modelling of skewness and kurtosis with two-piece scale and shape distributions. *Electronic Journal of Statistics*, 9(2):1884–1912, 2015.
- Richard L Smith. Statistics of extremes, with applications in environment, insurance, and finance. *Extreme Values in Finance, Telecommunications, and the Environment*, pages 20–97, 2003.
- Ignacio Vidal. A bayesian analysis of the gumbel distribution: An application to extreme rainfall data. *Stochastic Environmental Research and Risk Assessment*, 28(3):571–582, 2014.
- Ji Yae Shin, Si Chen, and Tae-Woong Kim. Application of bayesian markov chain monte carlo method with mixed gumbel distribution to estimate extreme magnitude of tsunamigenic earthquake. *KSCE Journal of Civil Engineering*, 19(2):366–375, 2015.
- Qingyang Liu, Xianzheng Huang, and Haiming Zhou. The flexible gumbel distribution: A new model for heavy-tailed data. *Manuscript submitted for publication*, 2022.

- John Geweke. Bayesian treatment of the independent student-t linear model. *Journal of applied econometrics*, 8(S1): S19–S40, 1993.
- Roger Koenker and Jose AF Machado. Goodness of fit and related inference processes for quantile regression. *Journal of the american statistical association*, 94(448):1296–1310, 1999.
- Jean Diebolt and Christian P Robert. Estimation of finite mixture distributions through Bayesian sampling. *Journal of the Royal Statistical Society: Series B (Statistical Methodology)*, 56(2):363–375, 1994.
- R Core Team. *R: A Language and Environment for Statistical Computing*. R Foundation for Statistical Computing, Vienna, Austria, 2022. URL <https://www.R-project.org/>.
- Mike Meredith, John Kruschke, and Maintainer Mike Meredith. Package ‘hdiinterval’. *Highest (Posterior) Density Intervals*, 2018.
- Aki Vehtari, Andrew Gelman, and Jonah Gabry. Practical bayesian model evaluation using leave-one-out cross-validation and waic. *Statistics and Computing*, 27(5):1413–1432, 2017.
- Bob Carpenter, Andrew Gelman, Matthew D Hoffman, Daniel Lee, Ben Goodrich, Michael Betancourt, Marcus Brubaker, Jiqiang Guo, Peter Li, and Allen Riddell. Stan: A probabilistic programming language. *Journal of Statistical Software*, 76(1), 2017.
- Keming Yu and Rana A Moyeed. Bayesian quantile regression. *Statistics & Probability Letters*, 54(4):437–447, 2001.
- Keming Yu and Jin Zhang. A three-parameter asymmetric laplace distribution and its extension. *Communications in Statistics—Theory and Methods*, 34(9-10):1867–1879, 2005.
- Robert Cichowicz, Grzegorz Wielgosiński, and Wojciech Fetter. Effect of wind speed on the level of particulate matter pm10 concentration in atmospheric air during winter season in vicinity of large combustion plant. *Journal of Atmospheric Chemistry*, 77(1):35–48, 2020.
- Joel Schwartz. Air pollution and hospital admissions for heart disease in eight us counties. *Epidemiology*, pages 17–22, 1999.
- Yaxue Zhao, Zhiyuan Cheng, Yongbin Lu, Xiaoyu Chang, Cynthia Chan, Yana Bai, Yawei Zhang, and Ning Cheng. Pm10 and pm2. 5 particles as main air pollutants contributing to rising risks of coronary heart disease: A systematic review. *Environmental Technology Reviews*, 6(1):174–185, 2017.
- D Isaacs, DG Altman, CE Tidmarsh, HB Valman, and AD Webster. Serum immunoglobulin concentrations in preschool children measured by laser nephelometry: Reference ranges for igg, iga, igm. *Journal of Clinical Pathology*, 36(10): 1193–1196, 1983.
- Fleur S van de Bovenkamp, Lise Hafkenscheid, Theo Rispens, and Yoann Rombouts. The emerging importance of igg fab glycosylation in immunity. *The Journal of Immunology*, 196(4):1435–1441, 2016.
- Patrick Royston and Douglas G Altman. Regression using fractional polynomials of continuous covariates: parsimonious parametric modelling. *Journal of the Royal Statistical Society: Series C (Applied Statistics)*, 43(3):429–453, 1994.
- Matthew D Hoffman, Andrew Gelman, et al. The No-U-Turn sampler: Adaptively setting path lengths in Hamiltonian Monte Carlo. *Journal of Machine Learning Research*, 15(1):1593–1623, 2014.
- Andrew Gelman, John B Carlin, Hal S Stern, David B Dunson, Aki Vehtari, and Donald B Rubin. *Bayesian Data Analysis*. CRC Press, 2013.
- Aki Vehtari, Andrew Gelman, Daniel Simpson, Bob Carpenter, and Paul-Christian Bürkner. Rank-normalization, folding, and localization: an improved r for assessing convergence of MCMC (with discussion). *Bayesian Analysis*, 16(2):667–718, 2021.



(a) Traceplots for the mean regression model



(b) Traceplots for the median regression model

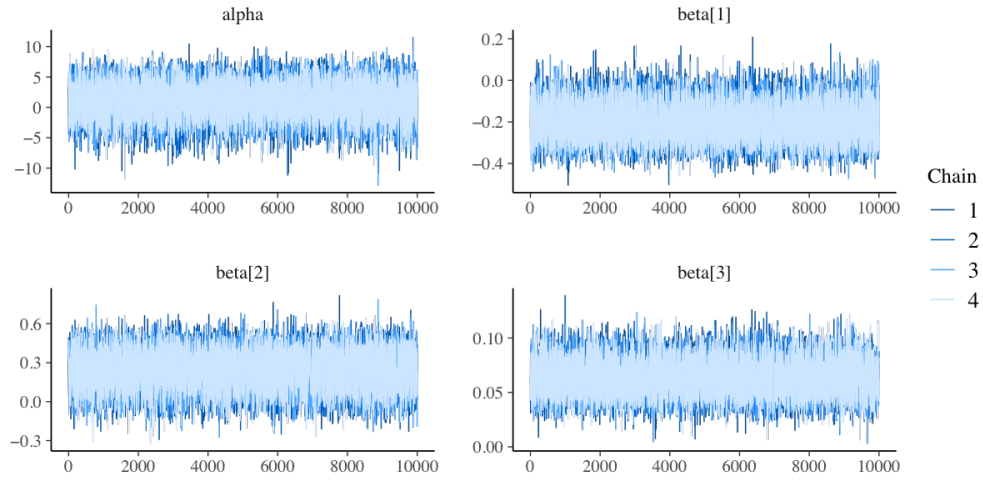
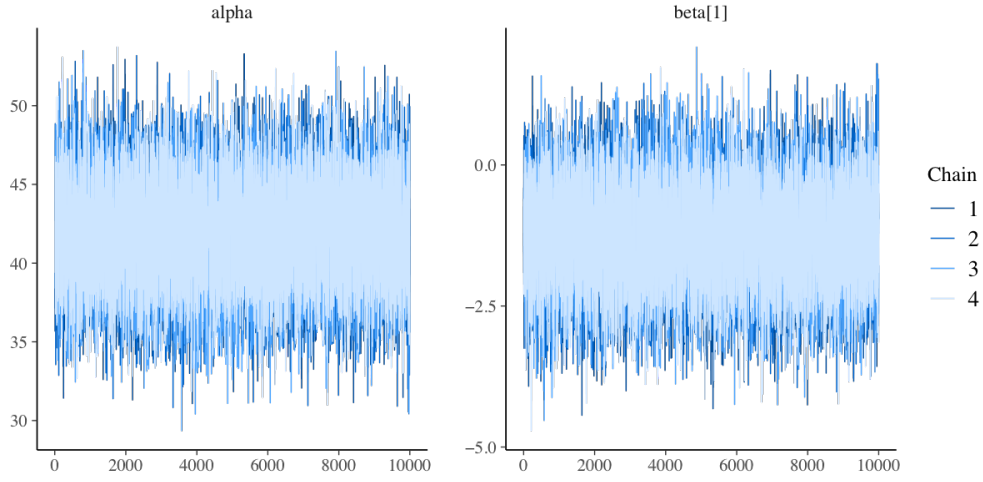
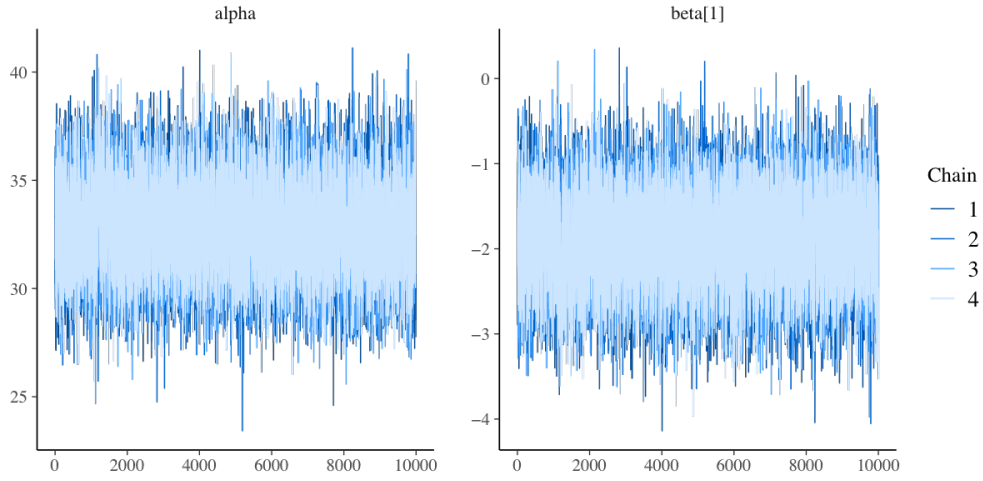
(c) Traceplots for the modal regression model based on the TPSC-Student- t likelihood

Figure 10: Traceplots for the mean/median/modal regression models fit to the crime data.



(a) Traceplots for the mean regression model



(b) Traceplots for the median regression model

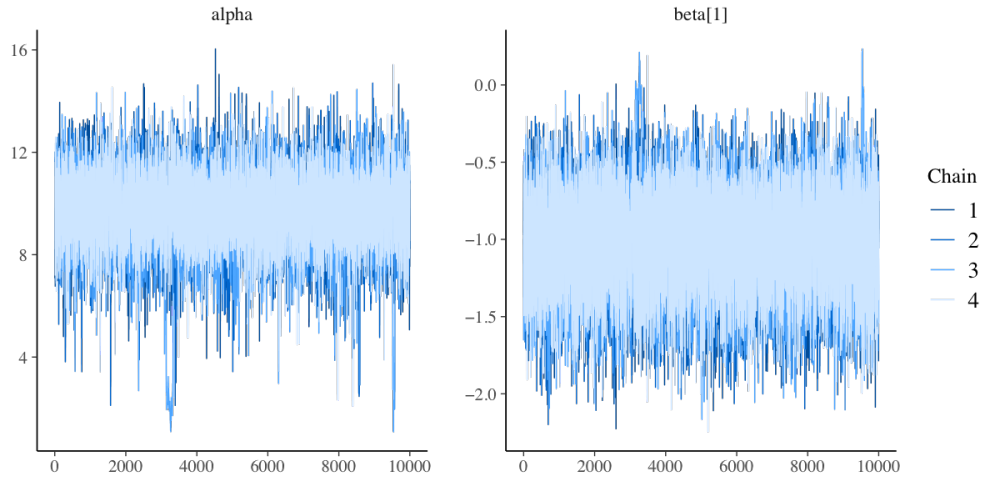
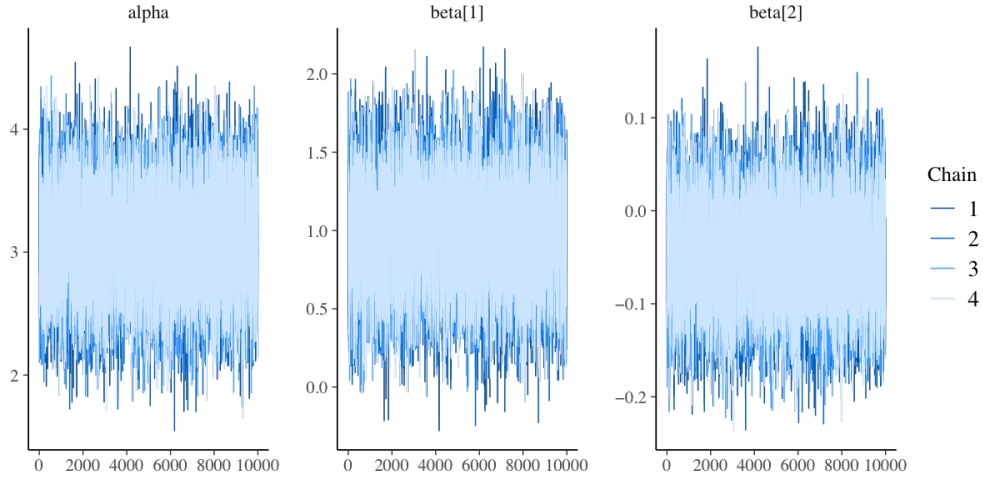
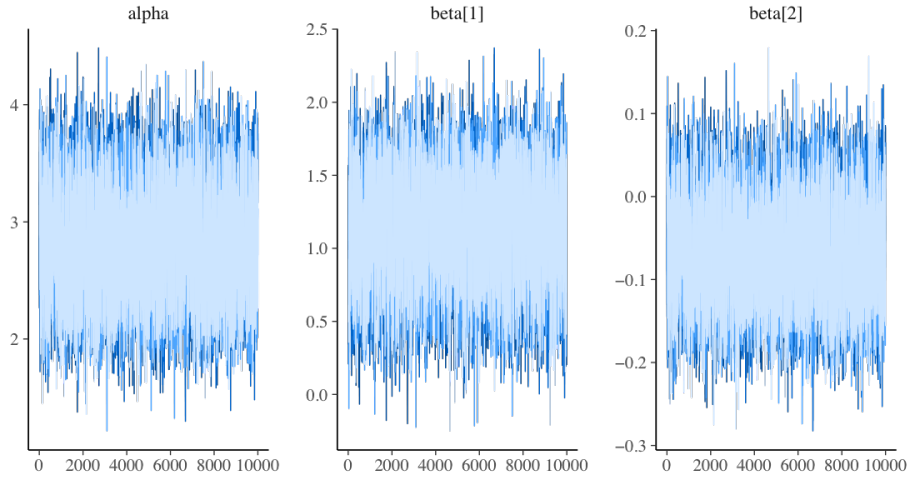
(c) Traceplots for the modal regression model based on the TPSC-Student- t likelihood

Figure 11: Traceplots for the mean/median/modal regression models fit to the air pollution data.



(a) Traceplots for the mean regression model



(b) Traceplots for the median regression model

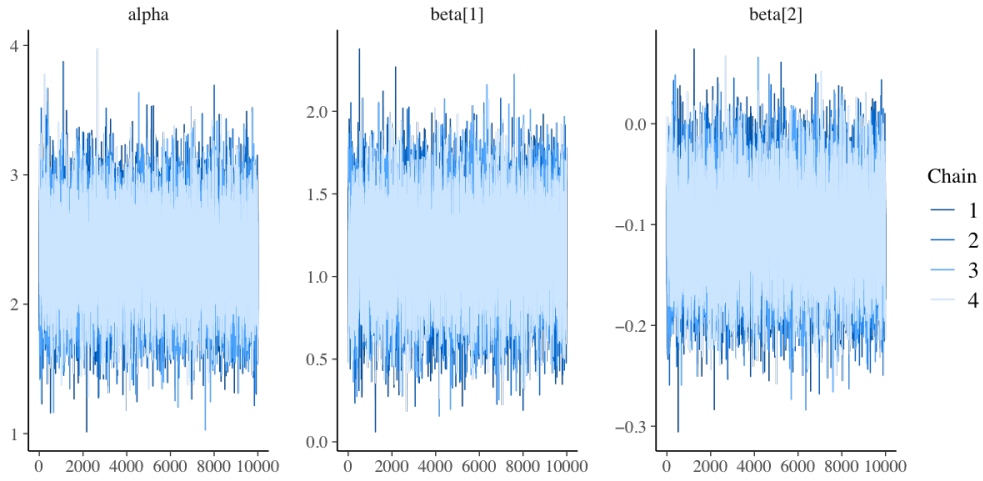
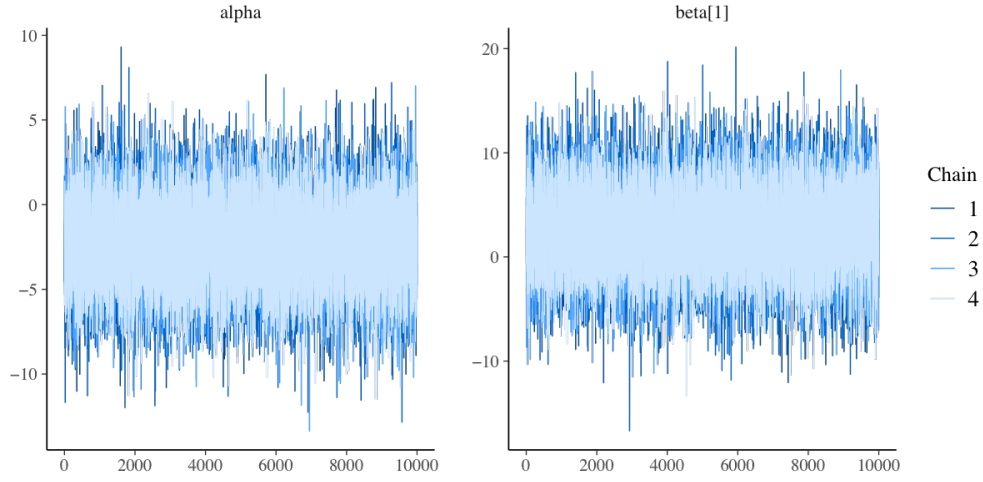
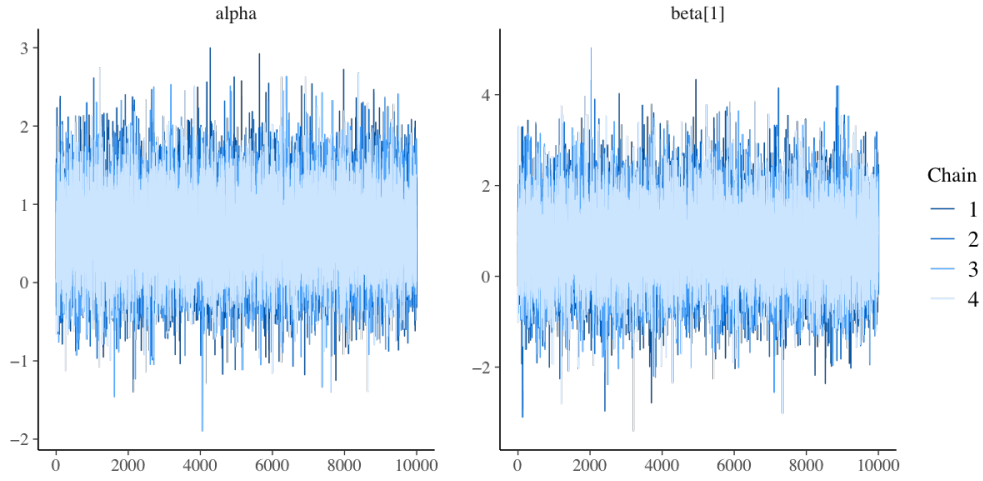
(c) Traceplots for the modal regression model based on the TPSC-Student- t likelihood

Figure 12: Traceplots for the mean/median/modal regression models fit to the serum data.



(a) Traceplots for the mean regression model



(b) Traceplots for the median regression model

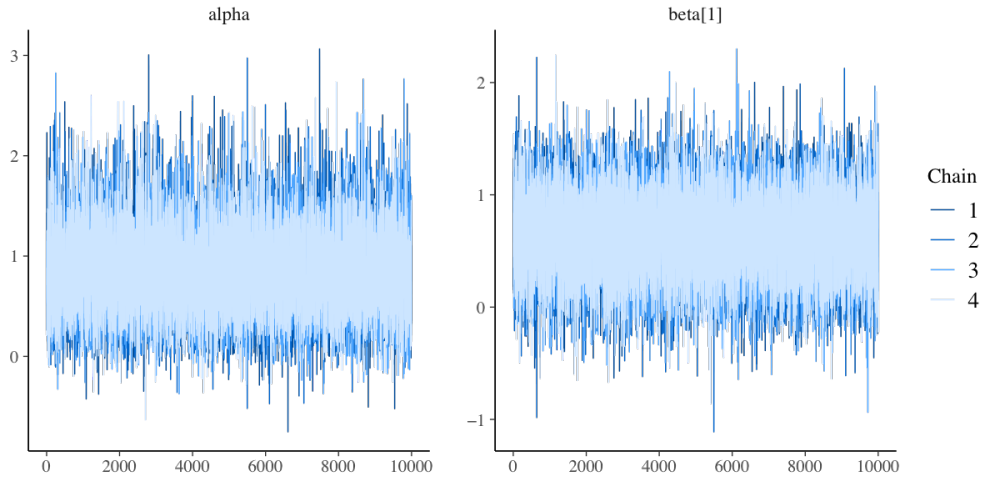
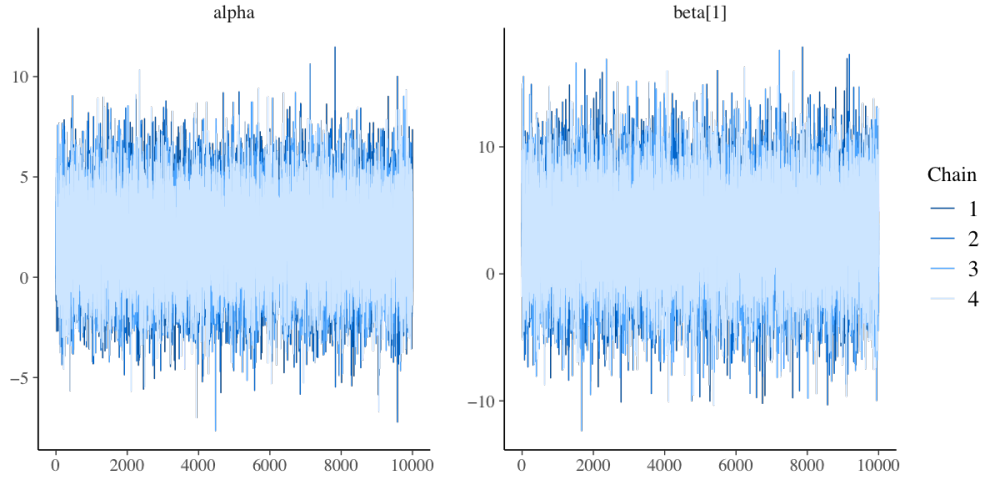
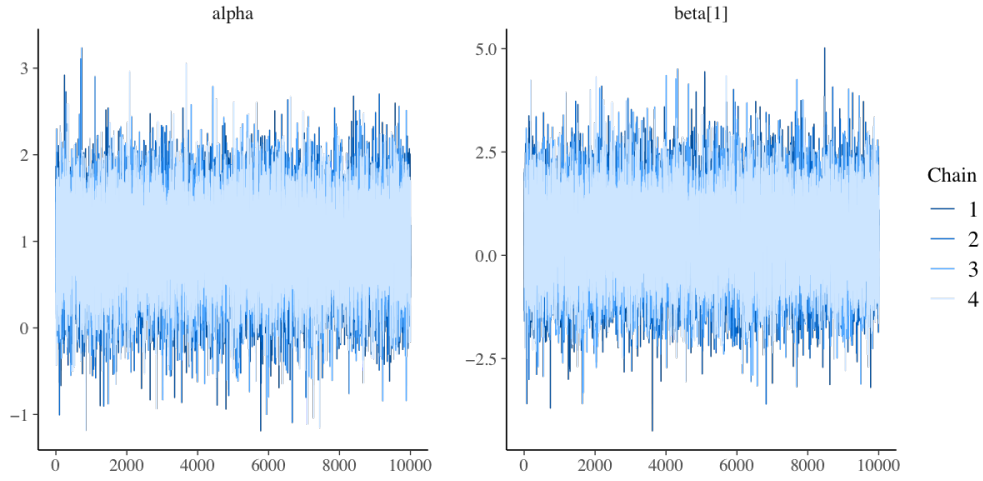
(c) Traceplots for the modal regression model based on the TPSC-Student- t likelihood

Figure 13: Traceplots for the mean/median/modal regression models from the left-skewed simulation study.



(a) Ttraceplots for the mean regression model



(b) Traceplots for the median regression model

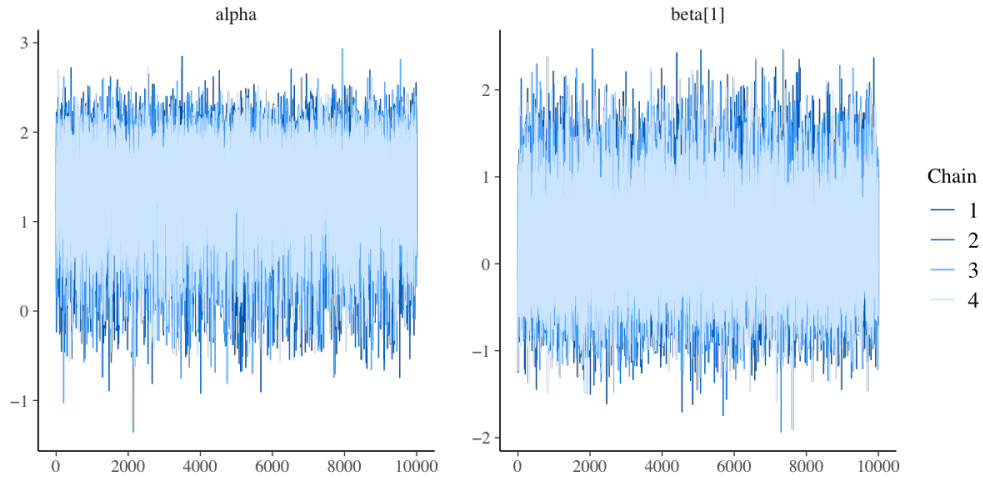
(c) Traceplots for the modal regression model based on the TPSC-Student- t likelihood

Figure 14: Traceplots for the mean/median/modal regression models from the right-skewed simulation study.